

**FABRICATION AND CHARACTERIZATION OF
MgB₂ POWDERS AND Cu-CLAD MgB₂ WIRES**

**A Thesis Submitted to
the Graduate School of Engineering and Sciences of
İzmir Institute of Technology
in Partial Fulfillment of the Requirements for the Degree of**

MASTER OF SCIENCE

in Physics

**by
Mert YAVAŞ**

**July 2005
İZMİR**

We approve the thesis of **Mert YAVAŞ**

Date of Signature



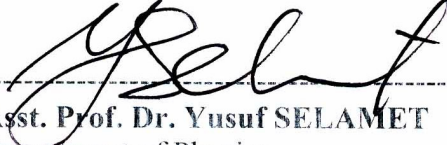
20 July 2005

Assoc. Prof. Dr. Salih OKUR
Supervisor
Department of Physics
İzmir Institute of Technology



20 July 2005

Prof. Dr. Kemal KOCABAŞ
Department of Physics
İzmir Dokuz Eylül University



20 July 2005

Asst. Prof. Dr. Yusuf SELAMET
Department of Physics
İzmir Institute of Technology



20 July 2005

Prof. Dr. Durmuş Ali DEMİR
Head of Department
İzmir Institute of Technology

Assoc. Prof. Dr. Semahat Özdemir
Head of the Graduate School

ACKNOWLEDGEMENTS

I am deeply grateful to Professor Durmuş Ali Demir for helping me throughout this thesis, making it possible against all odds and oddities.

There is no word to fully express the hope and support given me by my wife, Elif Dönertaş Yavaş.

And for their love and belief in me, Ünal Yavaş, Diler Yavaş and Zeynep Yavaş...

ABSTRACT

In 2001, a new superconducting material, MgB₂ (39K), which raised new hopes for electrical power applications due to its superior superconducting properties was discovered.

In the first part of this study, elementary B is obtained by reacting B₂O₃ and Mg in Argon atmosphere at 800°C. EDX results revealed that the powder obtained was Boron in 93% purity with Mg as a major impurity. MgB₂ is produced from acquired B and Mg in Ar atmosphere at 900°C by a conventional solid-state reaction. MgB₂ powders were pressed to a pellet at 500°C at 1 GPa. Microstructural properties of MgB₂ were determined by XRD, EDX, and SEM techniques. Electrical properties of fabricated MgB₂ were analyzed by resistivity measurements with closed-cycle cryopump system between 20 and 300K. It is found that the T_c onset value of the pellet is around 32K.

In the second part, different weight ratios of C is added to commercial MgB₂ and pressed at 500°C at 1 GPa. R-T measurements revealed that transition temperature increases with an increase in the C addition concentration.

In the third part, MgB₂/Mg composite wires were prepared by packing blend of MgB₂ and Mg powders inside Cu tubes using PIT method. The microstructure studies using XRD, EDX and SEM techniques showed that MgCu₂ layer forms at the interface between Cu sheath and core because of Mg diffusion from superconducting core, and excess Mg prevents further reaction of Cu with MgB₂. R-T measurements were performed to investigate the influence of excess Mg on T_c. The effect of annealing showed that excess Mg gives better results at annealing temperature of 400°C for 2 hours.

ÖZET

2001 yılında MgB_2 (39K) nin yeni bir üstüniletken olarak keşfi, üstüniletkenlik uygulamaları açısından umut verici olmuştur.

Bu çalışmanın ilk bölümünde elementer B, B_2O_3 ve Mg un $800^\circ C$ de Argon atmosferinde tepkimeye sokulması ile elde edilmiştir. EDX sonuçları elde edilen B un, %93 saflıkta olduğunu ve ana safsızlık olarak Mg un bulunduğunu ortaya koymuştur. Elde edilen B ve Mg $900^\circ C$ Ar atmosferinde, katı hal reaksiyonuna sokularak MgB_2 üretilmiştir. MgB_2 tozları $500^\circ C$ de 1 GPa basınç altında preslenerek tablete dönüştürülmüştür ve elektriksel karakterizasyonu kapalı devre cryopump sistemi ile 20 ve 300K arasında yapılmıştır ve tabletin T_c onset değerinin 32K civarında olduğu görülmüştür.

İkinci bölümde, farklı ağırlık oranlarında C, MgB_2 ye eklenmiş ve $500^\circ C$ de 1 GPa basınç altında basılmıştır. Direnç-Sıcaklık ölçümleri göstermiştir ki, üstüniletkenlik geçiş sıcaklığı, artan C yüzdesi ile artmaktadır.

Üçüncü bölümde, MgB_2 ve Mg tozlarının karışımı, Cu tüpler içerisine yerleştirilmiş ve daha sonra tüp içinde tel yöntemi kullanılarak MgB_2/Mg kompozit teller hazırlanmıştır. XRD, EDX ve SEM kullanılarak yapılan mikroyapısal çalışmalar, Cu kılıf ile üstüniletken merkez arasındaki arayüzeyde, merkezden Mg difüzyonu sebebiyle $MgCu_2$ katmanının oluştuğunu ve fazlalık Mg un Cu ile MgB_2 arasındaki başka bir reaksiyonu engellediğini ortaya koymuştur. Direnç-Sıcaklık ölçümleri, fazlalık Mg un kritik sıcaklık üzerindeki etkisini gözlemlemek üzere yapılmıştır. Fazlalık Mg un $400^\circ C$ de 2 saat tavllanmış örneklerde daha iyi sonuçlar gösterdiği bulunmuştur.

TABLE OF CONTENTS

LIST OF FIGURES	viii
LIST OF TABLES	xi
CHAPTER 1. INTRODUCTION	1
1.1 Historical Background	1
1.2 Basic Properties of Superconductors	3
1.3 Thesis Objectives	8
CHAPTER 2. PHYSICS OF SUPERCONDUCTOR MgB ₂	9
2.1 The Crystal Structure	9
2.2 Physics of Superconducting MgB ₂	10
2.3 Preparation of Bulk Samples from MgB ₂	18
2.3.1 Synthesis of MgB ₂	18
2.3.2 Metal Matrix Composite (MMC) Method	19
2.3.3 Powder In Tube (PIT) Method.....	20
CHAPTER 3. EXPERIMENTAL METHODS	23
3.1 Material Preparation.....	23
3.1.1 MgB ₂ Synthesis.....	23
3.1.2 Pellet Production	26
3.1.3 Powder in Tube Method (PIT).....	26
3.2 Characterization Methods	29
3.2.1 Four Point Probe Method.....	29
CHAPTER 4. RESULTS AND DISCUSSIONS	32
4.1 Elementary B and MgB ₂ Synthesis Results	32
4.1.1 Elementary B Synthesis Results	32
4.1.2 MgB ₂ Synthesis Results	34
4.2 C added MgB ₂ Pellet Production Results	37
4.3 Mg Added Cu Sheath MgB ₂ Wires Prepared by PIT Method Results	45

CHAPTER 5. CONCLUSIONS	51
REFERENCES	56

LIST OF FIGURES

<u>Figure</u>	<u>Page</u>
Figure 1.1. Schematic representation of Type I and Type II superconductors.....	4
Figure 1.2. Schematic representation of Cooper pair formation	5
Figure 2.1. The crystal structure of MgB ₂ , consisting Mg and B atoms	9
Figure 2.2. Temperature dependence of resistivity of MgB ₂	13
Figure 2.3. Hall coefficient of MgB ₂	14
Figure 2.4. Schematic representation of Powder In Tube Method.....	21
Figure 2.5. SEM Images of Fe clad tapes a) Transverse b) Longitudinal c) After Deformation d) After Annealing	22
Figure 3.1. A representation of the solid state reaction to produce elementary B powder	24
Figure 3.2. Purification process of B powder through Acid Leaching by HCl.....	24
Figure 3.3. MgB ₂ pellet production.....	25
Figure 3.4a. Representation of filling Cu tube with MgB ₂ powder	27
Figure 3.4b. Representation of hand pressing of MgB ₂ powder	27
Figure 3.5. Cold drawing Process.....	27
Figure 3.6. Cross-sectional view of Cu clad MgB ₂ wire.....	28
Figure 3.7. Annealing System	28
Figure 3.8. Four Probe Method	29
Figure 3.9. Closed Cycle Cryopump System	30
Figure 4.1. Variation of produced B purity with respect to acid leaching steps	33
Figure 4.2. XRD patterns of the powders before and after acid leaching of the powders obtained after the reaction of B ₂ O ₃ and Mg at 800°C	34
Figure 4.3. XRD patterns of the produced MgB ₂	35
Figure 4.4a. SEM image of produced MgB ₂ as powder.....	35
Figure 4.4b. SEM image of produced MgB ₂ as pellet.....	35
Figure 4.5. Temperature vs. Resistance plots of pellet pressed from MgB ₂ produced at IYTE and pellet pressed from commercial MgB ₂ (Alfa Aesar).....	36
Figure 4.6. Normalized Resistance vs. Temperature plots of pellet with 0% C addition to MgB ₂	39

Figure 4.7. Normalized Resistance vs. Temperature plots of pellet with 1% C addition to MgB ₂	39
Figure 4.8. Normalized Resistance vs. Temperature plots of pellet with 2% C addition to MgB ₂	40
Figure 4.9. Normalized Resistance vs. Temperature plots of pellet with 3% C addition to MgB ₂	40
Figure 4.10. Normalized Resistance vs. Temperature plots of pellets with 0%, 1%, 2% and 3% C addition to MgB ₂ with applied current 0.1 mA	41
Figure 4.11. Normalized Resistance vs. Temperature plots of pellets with 0%, 1%, 2% and 3% C addition to MgB ₂ with applied current 0.5 mA	42
Figure 4.12. Normalized Resistance vs. Temperature plots of pellets with 0%, 1%, 2% and 3% C addition to MgB ₂ with applied current 1 mA	42
Figure 4.13. Normalized Resistance vs. Temperature plots of pellets with 0%, 1%, 2% and 3% C addition to MgB ₂ with applied current 2 mA	43
Figure 4.14. Normalized Resistance vs. Temperature plots of pellets with 0%, 1%, 2% and 3% C addition to MgB ₂ with applied current 3 mA	43
Figure 4.15. Normalized Resistance vs. Temperature plots of pellets with 0%, 1%, 2% and 3% C addition to MgB ₂ with applied current 5 mA	44
Figure 4.16. Normalized Resistance vs. Temperature plots of pellets with 0%, 1%, 2% and 3% C addition to MgB ₂ with applied current 10 mA	44
Figure 4.17. SEM micrograph of cross section of an annealed Cu-sheathed MgB ₂ + 5% Mg composite wire with 1.5 mm in diameter. (on the left).....	46
Figure 4.18. EDX Intensity has taken at the interface between Cu sheath and MgB ₂ + 5% Mg core while moving along the radial direction toward to the core center as shown in Figure 4.17. The sample was prepared after cold drawing process and annealing at 800°C for 3 min. (on the right)	46
Figure 4.17. The sample was prepared after cold drawing process and annealing at 800°C for 3 min. (on the right)	46

Figure 4.19. X-ray diffraction patterns of the MgB ₂ powders, a) before packing, b) of the MgB ₂ filament after removing the Cu sheath mechanically after the cold drawing process to a wire with outer diameter of 1.5 mm, c) after annealing at 800 °C for 3 min., d) of the mixed MgB ₂ filament with 5% Mg before annealing, e) of the 5% Mg added filament after annealing at 800 °C for 3 min., f) of the mixed MgB ₂ filament with 10% Mg before annealing, and g) of the 10% Mg added filament after annealing at 800 °C for 3 min	47
Figure 4.20. X-ray diffraction patterns a) of the MgB ₂ (pure) filament of the Cu-clad MgB ₂ wire after annealing at 400°C for 2 h, b) of the 5% Mg added filament after annealing at 400°C for 2 h, c) of the 10% Mg added filament after annealing at 400°C for 2 h.....	48
Figure 4.21. R-T characteristics of sintered and un-sintered MgB ₂ wires with Cu sheath material at a driven current of 50 mA	49

LIST OF TABLES

<u>Figure</u>		<u>Page</u>
Table 2.1.	The recent status of critical current density (J_c) of MgB_2	15
Table 2.2.	Effects of additives on J_c of MgB_2 at 20 K.....	16
Table 4.1.	Weight percentage of the elements before and after acid leaching	33
Table 4.2.	Densities of the pellets with 0%, 1%, 2% and 3% C addition to MgB_2	37
Table 4.3.	Transition temperatures of the pellets with 0%, 1%, 2% and 3% C addition to MgB_2	38

CHAPTER 1

INTRODUCTION

Superconductivity is the ability of some materials to conduct electric current with practically zero resistance. It was discovered by Kammerlingh Onnes in 1911 in pure mercury (4.2 K) (Onnes 1911). Since then, this discovery which raised new hopes for applications in magnet and energy technology triggered plenty of interest. Scientists did many researches to understand the theoretical background of this phenomenon. They looked for to find new superconducting materials, and also developed and enhanced the properties of existing superconductor technology. As a result of this intense research, recently a new superconductor material, $\text{HgBa}_2\text{Ca}_2\text{Cu}_3\text{O}_8$, which has a critical temperature of 133 K is reported. Although there are several superconducting materials which have a transition temperature above the boiling point of liquid nitrogen (77 K), some of their structural and superconducting properties prevented them to be commercialized extensively. Consequently 99% of today's technology of superconductor applications are dependent on Nb based superconductors materials with a transition temperature below 20 K. Discovery of MgB_2 (Nagamatsu et al. 2001) received considerable attention of scientists owing to its 39 K transition temperature and latest studies revealed that MgB_2 is a future promising candidate to reform existing superconductor industry which is based on Nb based superconductors, Nb_3Sn (18 K) specifically.

1.1 Historical Background

Superconductors, materials that have no resistance to the flow of electricity below a certain critical temperature (T_c), are one of the most exciting scientific discoveries.

Dutch physicist Heike Kamerlingh Onnes of Leiden University was working on He liquefaction techniques (1908) and in 1911 he succeeded to cool Hg to the temperature of liquid He, 4 degrees Kelvin, and its resistance suddenly dropped to zero at 4.2K, a phase transition to a zero resistance state. He investigated the low temperature

resistivity of mercury, as mercury could be made very pure by distillation, and this was important because the resistivity at low temperatures tends to be dominated by impurity effects. Later, in 1913, he won a Nobel Prize in physics for his research in this area.

The next milestone in understanding how matter behaves at extreme cold temperatures occurred in 1933. Walter Meissner and Robert Ochsenfeld discovered that when a material makes the transition from the normal to superconducting state, it actively excludes magnetic fields from its interior (Meissner and Ochsenfeld, 1933). A conductor will oppose any change in externally applied magnetic field. Circulating currents will be induced to oppose the buildup of magnetic field in the conductor (Lenz's law). In a solid material, this is called diamagnetism, and a perfect conductor would be a perfect diamagnet. That is, induced currents in it would meet no resistance, so they would persist in whatever magnitude necessary to perfectly cancel the external field change. This phenomenon is referred to as the "Meissner effect". The Meissner effect is so strong that a magnet can actually be levitated over a superconductive material.

The disappearance of electrical resistivity was modeled in terms of electron pairing in the crystal lattice by John Bardeen, Leon Cooper, and Robert Schrieffer in what is commonly called the BCS theory (Bardeen et al. 1957). They received the Nobel Prize in 1972 for the development of the theory of superconductivity.

From the discovery of superconductivity till today scientists have been trying to find new superconducting materials with high critical temperatures. Several materials with respect to an increase in the T_c can be counted as: metals and intermetallic compounds with up to 23.2 K (Hg, Pb, Nb based superconductors), (Testardi et al. 1974, Gavaler et al. 1974), (La,Ba)CuO₄ system with 35 K (Bednorz and Mueller 1986), in 1987 YBa₂Cu₃O₇ with 93 K, and finally HgBaCaCuO with a T_c of 130 K is reported. A new era in the study of superconductivity began with the discovery of high critical temperature superconductors in 1986, as liquid nitrogen could be used to cool down the superconductors. Some necessary requirements should be fulfilled, for these superconductor materials to be widely used in commercial applications. The first, maybe the most important one is T_c , but the material should also grant to be useful by both the superconducting and structural properties. This is the main reason why; although higher T_c superconductor materials were found, they could not be used and Nb based superconductors dominate the conventional superconductor technology today. As for metals and intermetallic compounds the highest T_c is 23.2 K with Nb₃Ge, and

YPd₅B₃C_{0.3} (Cava et al. 1994) the discovery of MgB₂ with a T_c of 39 K is future promising to replace Nb based superconductor technology. Since then studies to understand the mechanism of superconductivity in MgB₂ support the convenience of this material for this technology.

1.2 Basic Properties of Superconductors

One of the important properties of superconductors is T_c the critical temperature at which the resistivity of the material vanishes. Many researches aimed to find new superconducting materials with high critical temperatures. Another important parameter is critical magnetic field (H_c). Superconducting state cannot exist in the presence of an applied magnetic field greater than a critical value called H_c even at absolute zero. This critical magnetic field which is a characteristic of the material is strongly correlated with the critical temperature of the superconductor. T_c decreases with the increase in H_c. According to Meissner effect, the magnetic field lines are expelled from the sample when it is in superconducting state. The external field penetrates into the bulk from the surface of the sample, but the magnitude of the magnetic field that penetrates decreases, exponentially. The maximum penetration possible is called the penetration depth. It is given in the penetration depth formula where x is the distance from the surface, and λ is the penetration depth.

$$H(x) = H_0 \exp(-x/\lambda) \quad 1.1$$

According to their diamagnetic properties superconductors categorized into two groups, type I and type II. In type I superconductors, H_c is a limiting factor because when the applied magnetic field is increased, the magnetization balancing this magnetic field also increases until H_c is reached. The material leaves its superconducting state if the magnetic field applied from outside surpasses H_c. When the applied magnetic field is lower than H_c, the material is in the Meissner state. In this state all magnetic flux is expelled from the sample. Type I superconductors which are mostly pure metals have been of limited practical usefulness because the critical magnetic fields are so small and the superconducting state disappears suddenly at that temperature.

In Type II Superconductors on the other hand, change from the normal state to Meissner state doesn't occur immediately but goes through a transitional state in which the applied field is able to penetrate through certain local regimes of the sample. This is called the vortex state because vortices of superconducting currents surround filaments or cores of normal material, and it shows the properties of a mixed state of normal and superconducting regions. If the applied magnetic field is increased until the lower critical field, H_{c1} , is reached, the material expels all the magnetic flux that falls on it. If the applied magnetic field is kept on being increased, until upper critical field, H_{c2} , the material is in the vortex state and magnetic flux lines can penetrate through the sample in some regions. The effect of these flux lines are cancelled out by the supercurrents circulating around the walls of vortices and the total magnetic flux is zero.

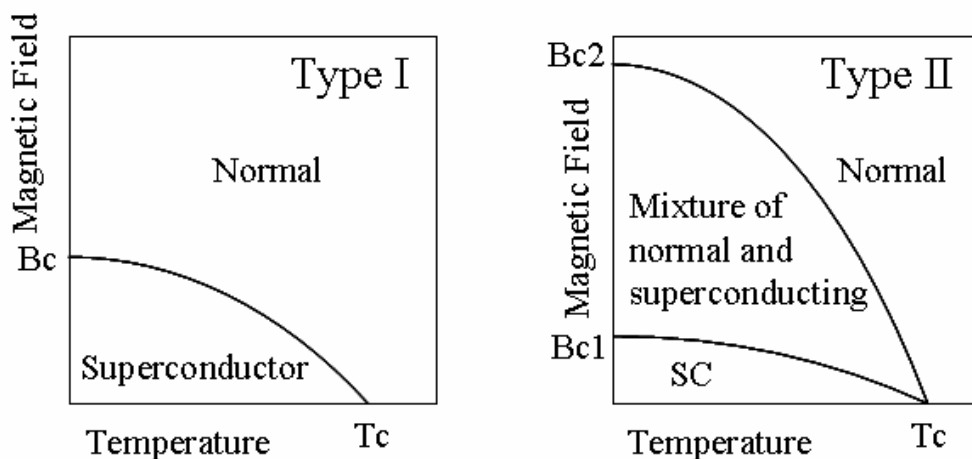


Figure 1.1. Schematic representation of Type I and Type II superconductors

Most of Type II superconductors are alloys and they exhibit much higher critical magnetic fields.

Other than H_c there is another important parameter affecting the quality of the superconductor which is J_c , critical current density. J_c , the maximum current the material can carry per unit area, is strongly dependent on temperature. As the current flowing through a superconductor increase, T_c will usually decrease. The current through a superconductor creates a magnetic field, when the current density is high

enough, the magnetic field at the surface of the sample becomes larger than the critical magnetic field (H_c) and the superconductivity vanishes.

In 1957, Bardeen, Cooper and Schrieffer (BCS) proposed a theory that explained the microscopic origins of superconductivity, and could quantitatively predict the properties of superconductors. (Bardeen et al. 1957) BCS theory relies on an earlier discovery by Cooper (1956), who showed that the ground state of a material is unstable with respect to pairs of 'bound' electrons. These pairs are known as Cooper pairs and are formed by electron-phonon interactions. An electron in the cation lattice will distort the lattice around it, creating an area of greater positive charge density around itself. Another electron at some distance in the lattice is then attracted to this charge distortion (phonon). This is the electron-phonon interaction. The electrons are thus indirectly attracted to each other and form a Cooper pair namely, an attraction between two electrons mediated by the lattice which creates a 'bound' state of the two electrons. Pairs of electrons can behave very differently from single electrons which are fermions and must obey the Pauli Exclusion Principle. The pairs of electrons act more like bosons which can condense into the same energy level and possess one single wave function describing the behaviours of all Cooper pairs.

Bardeen, Cooper, and Schrieffer received the Nobel Prize in 1972 for the development of the theory of superconductivity.

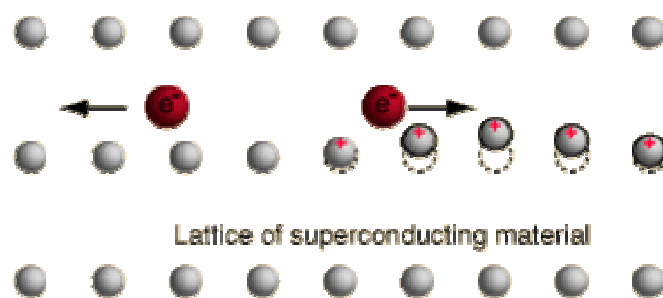


Figure 1.2. Schematic representation of Cooper pair formation

The BCS Theory explains the mechanism of superconductivity in low temperature superconductors. It has an estimation of 30 K as the highest T_c a superconductor can achieve so therefore unable to explain high temperature superconductors with much higher T_c values. Transition temperature of 39 K in newly discovered MgB_2 is announced to be also explained by BCS theory in most recent publications. (Zhao 2002)

The main issue to be solved for the superconductor technology to be commercialized is cooling the system. A broad range of superconducting devices have been proposed but their widespread usage is possible only through a discovery of new superconducting materials with transition temperatures on the range of room temperature. Therefore the realization of high temperature superconductors raised new hopes for many more applications. Although there is an increase in the transition temperature with high T_c superconductors, cooling still remains to be a drawback to be overcome.

There are three main regimes that superconductors are inclined to work in. These regimes are based on the zero resistance when superconducting state is maintained, transition between the superconducting state and normal state and Josephson Junctions.

Superconducting magnets can be regarded as the main applications in the regime of zero resistance. When the requirement in question is producing high magnetic fields, superconducting wires wound up for kilometers to produce solenoids, is the right choice. Superconducting magnets are recently used primarily in medical and scientific instrumentation namely MRI (magnetic resonance imaging) and particle accelerators. In many other applications where attainability of high currents is not crucial, instead of wires, superconductor films are used.

Other bulk applications of superconductors that focus on the low frequency magnetic properties include magnetic levitation MAGLEVS, magnetic bearings and magnetic shielding.

Some of the applications that are still being developed are lossless transmission structures and microwave filters using the advantage of superconductors to show very small resistance at radio (RF) and microwave frequencies.

The low resistance of superconductors included in microwave circuits results in many desirable properties useful in applications such as sharp skirt filters, delay lines, high Q resonators, cavities and antennas (Heinen and Bhasin 1991).

A superconductor with a sharp transition (or small ΔT), being held at the transition interval, can be used as thermal detectors and switches. Resistance can be significantly altered with a small influence of temperature. This prepares the working principle of the bolometer and switches which are rather sensitive to thermal or optical energy changing.

Superconducting quantum interference devices (SQUID) which are made up of Josephson junctions are the most widely applied of low temperature superconducting devices. They are the essential core component in the most sensitive magnetometers, but they are also used in voltmeters, amplifiers and motion detectors. Applications include the measurement of magnetic activity in the human brain inside magnetically screened rooms with arrays of spatially sensitive SQUID detectors, and measurement of motion predicted in gravity waves from collapsing stars. Moreover, there is a widespread need for sensitive magnetic measurements in geological studies, but the cryogenic complexity of low temperature SQUIDs has so far precluded them.

As we have considered the general applications of superconductors, now we can take a closer look at the application areas of MgB_2 .

99% of today's superconductor technology is dependent upon low T_c superconductors which are Nb based intermetallic compounds. Although these materials have low transition temperature, they are easy to produce and are convenient for commercial purposes. On the other hand, MgB_2 has a T_c value of 39K which is almost twice as much of Nb_3Ge (23K) and a lot higher than other superconductor materials which are mostly used in superconductor technology today such as $NbTi$ (9K) and Nb_3Sn (18K). MgB_2 has high critical current density and resist to high critical fields (B_{c2}). It also has large coherence length (Buzea and Yamashita 2001), (Bud'ko et al. 2001) with a simple crystal structure. As it has low anisotropy, it is easy to fabricate wires using MgB_2 . Mechanism of superconductivity can be explained by using BCS Theory and therefore the occurrence is not so difficult to explain like in the case of high T_c superconductors. This is the reason why MgB_2 with a transition temperature of 39K has an advantage over the current superconductor technology and it is hoped that it will be an efficient replacement for applications using both MgB_2 wires and films.

1.3 Thesis Objectives

The recent discovery of MgB_2 as a superconductor with transition temperature of 39K has promoted significant attention in the area of fundamental and applied research on superconducting materials, globally. MgB_2 has simple crystal structure, large coherence length, high critical fields (B_{c2}), and high transport critical current densities (J_c) have been reported in MgB_2 bulk samples. Due to its intermediate transition temperature, weak-link free grain boundaries (Glowacki et al. 2001) and low material cost, this material is appealing for potential applications such as MRI and transformers at operating temperature of 20-30K.

In this thesis our objective is to fabricate and characterize MgB_2 powders and Cu-clad MgB_2 wires. To prepare MgB_2 we used several processes namely elementary B production, B purification and finally MgB_2 synthesis. Then to produce pellets we used hot pressing technique. To see the effect of C addition to pellets, 0% C, 1% C, 2% C, 3% C added pellets were prepared. In literature there is no study explaining C addition, but there are many studies about C doping or C substitution. These studies state that C doping decreases the transition temperature of MgB_2 with respect to increasing C content but on the other hand there is an enhancement in the magnetic properties of the C doped MgB_2 . There is not a chance of comparison of our C added pellets with literature as the preparation methods are very different from each other. For the production of wires we used Powder-In-Tube (PIT) method. In this study Mg addition to MgB_2 wires were also covered. Mg is chosen as the metal matrix because of its low melting point (653°C) and its inertness to MgB_2 at very high temperatures. (Dunand 2001)

To characterize the electrical and microstructural properties of the samples prepared, we used a closed-cycle He cooled cryopump system (20-300K) for the R-T measurements, Scanning Electron Microscopy (SEM), together with Energy Dispersive X-ray Spectroscopy (EDX) and X-ray Diffraction Spectroscopy (XRD).

CHAPTER 2

PHYSICS OF SUPERCONDUCTOR MgB_2

2.1 The Crystal Structure

MgB_2 is an “old” material, known since early 1950’s, but only recently discovered to be a superconductor at a remarkably high critical temperature about 40 K. The most appealing property of MgB_2 seems to be its high T_c but its popularity is also due to its simple hexagonal structure.

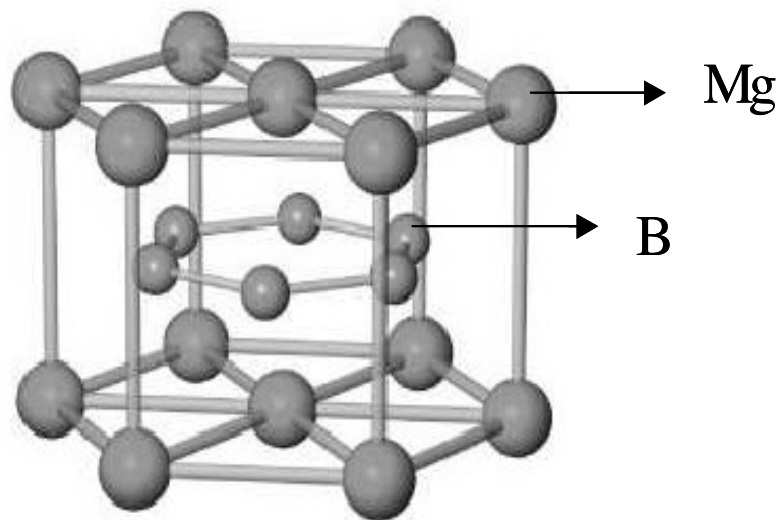


Figure 2.1. The crystal structure of MgB_2 , consisting Mg and B atoms. (Larbalestier et al. 2001a)

It has a hexagonal AlB_2 type crystal structure, where the B atoms form graphite like sheets separated by hexagonal layers of Mg atoms (Yildirim 2002). Lattice constants are $a=3.086 \text{ \AA}$ and 3.524 \AA .

2.2 Physics of Superconducting MgB₂

Superconductivity, since it was found by Onnes in 1911, has been studied both experimentally to find new superconducting materials with high transition temperatures and theoretically to explain the physical phenomena beneath superconductivity. The most accepted theory to explain superconductivity is formulated by Bardeen, Cooper and Schreiffner, and is called BCS theory. A key conceptual element in this theory is the pairing of electrons close to the Fermi level into Cooper pairs through interaction with the crystal lattice. This pairing result from a slight attraction between the electrons related to lattice vibrations; the coupling to the lattice is called a phonon interaction. BCS theory is mainly capable of explaining Type I superconductors which have low T_c values.

If electrical conduction in superconductor materials were purely electronic, there should be no dependence upon the nuclear masses. Isotope effect was observed as the dependence of the critical temperature for superconductivity upon isotopic mass and it was the first direct evidence for interaction between the electrons and the lattice, and this supported the BCS theory of lattice coupling of electron pairs. It is quite remarkable that an electrical phenomenon like the transition to zero resistivity should involve a purely mechanical property of the lattice. Since a change in the critical temperature involves a change in the energy environment associated with the superconducting transition, this suggests that part of the energy is being used to move the atoms of the lattice since the energy depends upon the mass of the lattice. This indicates that lattice vibrations are a part of the superconducting process. This was an important clue in the process of developing the BCS theory because it suggested lattice coupling, and that phonons were involved.

Isotope effect is formulated, as α representing the isotope effect coefficient, as follows:

$$\alpha = -\frac{d \ln T_c}{d \ln M} \approx -\left(\frac{M}{\Delta M}\right)\left(\frac{\Delta T_c}{T_c}\right) \quad 2.1$$

For the total reduced isotope effect coefficient of a system made up of multiple components, the formula is the following:

$$\alpha_{total} = \sum \alpha_i = \sum \frac{-d \ln T_c}{d \ln M} \quad 2.2$$

Isotope effect is an indication of phonon mediated superconductivity and therefore it is experimental evidence to support BCS explanation. Consequently isotope effect to be observed in superconducting MgB₂ is a salient guide to understand the physics of this material.

Isotope effect in MgB₂ was first examined by Bud'ko et al. (Bud'ko et al. 2001a). He and his colleagues worked with different isotopes of boron atom, namely ¹⁰B, and ¹¹B. They found that there was an increase in the critical temperature and the isotope effect coefficient for B was $\alpha=0.28$. Another significant study by Hinks (Hinks et al. 2001) revealed the isotope effect in Mg and B and the isotope effect coefficient for Mg was $\alpha=0.02$ and for B was 0.30. Hinks also suggested that the total reduced isotope-effect coefficient is 0.32. Also an important result of this study is that the phonons of B atom contribute more to the pairing mechanism in superconductivity of MgB₂ than Mg atoms do. MgB₂ is special among high T_c superconductors because both Mg and B are light elements having stable isotopes. That is why isotope effect in MgB₂, can be properly measured. As a result of these studies because the total reduced isotope effect coefficient of MgB₂ is found to be smaller than 0.5, it is said that MgB₂ is a BCS type superconductor. There are two main reasons for the reduced isotope effect coefficient of MgB₂ to be smaller than the ideal value BCS theory predicts. These can be summarized as strong coulomb repulsion (Lorenz et al. 2001), and large anharmonicity, in the vibrations of B atoms (Bordet et al. 2001). Lattice becomes stiffer when the pressure in the medium increases resulting in the decrease in the transition temperature of MgB₂. This behavior is often observed in BCS type superconductors.

Apart from the isotope effect another significant property of MgB₂, is that it is one of the clearest examples of two gap superconductors ever studied.

The postulation of two-gap superconductivity in MgB₂ was proved from the band calculations theoretically (Liu et al. 2001, Choi et al. 2002). Several studies revealed similar results and these can be summarized as: (Naito and Ueda 2004).

1. Mg is substantially ionized, and MgB_2 can be well described as the ionic form $\text{Mg}^{2+}(\text{B}_2)^{2-}$.
2. The band near the Fermi level is mainly derived from the distinct sets of boron orbitals: $sp^2(\sigma)$ states and $p_z(\pi)$ states. The σ bands are 2D in character and form cylindrical Fermi surfaces, whereas the π bands have more of a 3D character owing to a substantial c-axis transfer integral and form 3D tubular networks of Fermi surfaces.
3. The σ bands (2D FS) interact strongly with the E_{2g} phonon mode and are predicted to have a large 2D superconducting gap. However, the π bands have weaker electron–phonon interaction and their superconducting gap is about 3 times smaller in magnitude.

Experimental indication of the two band superconductivity was observed through several spectroscopic methods as tunneling, point contact, photoemission, far-infrared optics and also temperature dependence of specific heat, microwave surface resistance and penetration depth at low temperature methods, to determine the superconducting energy gap of MgB_2 . (Buzea and Yamashita 2001, Schmidt et al. 2001).

It was found that the Fermi surface consists of two tubular networks. These networks arose from two nearly cylindrical sheets from the two-dimensional σ bands and from three-dimensional π bonding and antibonding bands. These four bands are usually considered as two effective bands because of their contribution to superconducting behavior of the material. Superconductivity occurs by the effect of strong electron-phonon coupling in the 2D σ bands and the reason of superconducting behavior of the π electrons is their interband coupling to σ electrons. Consequently, there are two distinct energy gaps, 2D band showing a large gap, $\Delta_\sigma \sim 7\text{-}8$ meV, on the other hand the 3D band having a small gap $\Delta_\pi \sim 2\text{-}3$ meV. Both gaps closes at the same critical temperature $T_c = 39$ K (Liu et al. 2001, Choi et al. 2002, Bouquet et al. 2001).

The basic physical properties of MgB_2 are worth mentioning in this part of this thesis. The first parameter is the resistivity of MgB_2 . The studies about resistivity of MgB_2 can be studied under two sections. The first section covers information about the resistivity of MgB_2 while the samples studied were polycrystalline in nature. The reported values for the resistivity are different from group to group (from 100 m Ω -cm to 0.3 $\mu\Omega$ -cm) (Rowell 2003). The second section covers information about the resistivity

of MgB_2 while the samples studied were single crystals or crystalline films. Single crystals were produced by using high-pressure furnaces or single crystalline films were produced by using a two-step method (Tu et al. 2001). In this case the reported values for resistivity are more consistent. The resistivity value of MgB_2 at room temperature is approximately $5\text{-}6 \mu\Omega\text{-cm}$. Figure 2.2, which can be compared to $\rho(300 \text{ K})$ of nearly $2 \mu\Omega\text{-cm}$ for Cu, $\sim 15 \mu\Omega\text{-cm}$ for Nb, $\sim 80\text{-}\mu\Omega\text{-cm}$ for Nb_3Sn and $150 \mu\Omega\text{-cm}$ for $\text{YBa}_2\text{Cu}_3\text{O}_x$. The low temperature resistivity value of MgB_2 is between $0.3 \mu\Omega\text{-cm}$ and $3 \mu\Omega\text{-cm}$ (Rowell 2003, Bud'ko et al. 2001b). The reason for this large variation is explained by the amount of the impurity scattering, stoichiometry variations and porosity (Rowell 2003, Sharma et al. 2001).

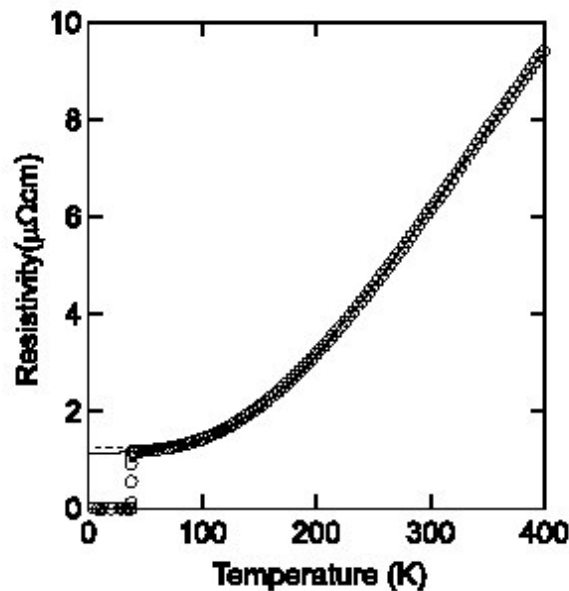


Figure 2.2. Temperature dependence of resistivity of MgB_2 . (Source: Masui and Tajima 2003)

The second parameter to give information about is the hall coefficient R_H . For MgB_2 , there are four bands near Fermi level. Two of these bands are hole like σ bands forming 2D cylindrical Fermi surfaces. The other two bands are hole and electron like 3D π bands in the band structure of MgB_2 . Due to this multi band structure of MgB_2 , the hall coefficient shows strong anisotropy as seen in Figure 2.3 (Masui and Tajima 2003). In $H \parallel c$, the hole like carriers dominate the behavior of R_H , and give positive values of

R_H . When magnetic field (H) is applied parallel to the ab plane, the σ bands became less important, and electron like carriers dominate the R_H . Due to the fact that MgB_2 is a superconductor which has multi band structure, the absolute value of the R_H is not the direct measure of the carrier density. The carrier densities are estimated to be $n \sim 3.4 \cdot 10^{22} \text{ cm}^{-3}$ and $p \sim 2.6 \cdot 10^{22} \text{ cm}^{-3}$ at 40 K in single crystalline samples (Eltsev et al. 2001). The absolute values of R_H are about one order larger than R_H in polycrystalline samples (Kang et al. 2001) and in thin films (Kang et al. 2002). This difference can be explained by the compensation between the positive and negative components due to the randomly oriented grains. In Figure 2.3 both R_H values show substantial temperature dependence. This situation can be explained by different T dependence of scattering rate for different bands.

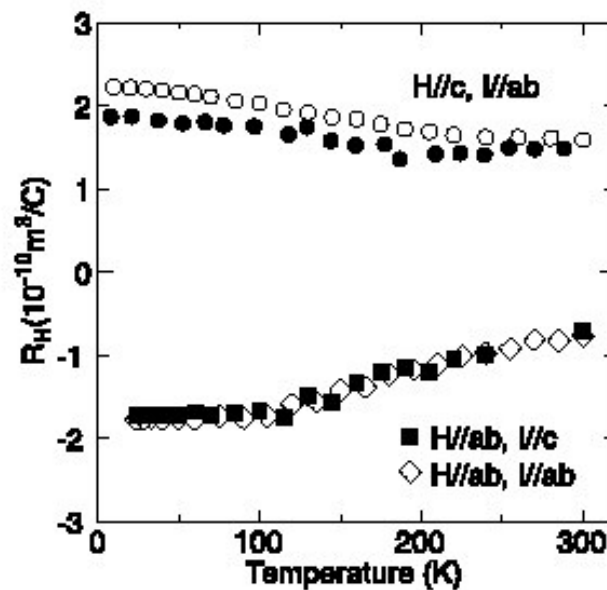


Figure 2.3. Hall coefficient of MgB_2 . (Source: Masui and Tajima 2003)

The discovery of superconductivity at 39 K in MgB_2 (2001) has created great interests worldwide in both fundamental studies and practical applications. As the critical temperature of this material is well above 20 K, the temperature for superconductor applications in today's market, it is a potential candidate for several applications in industry. But on the point of engineering view besides operating at relatively high temperature, a superconducting device should also be able to operate in a

sufficiently high magnetic field. The current status of the critical current densities of MgB₂ superconductor in different magnetic fields for wire, tape, bulk and thin film samples are summarized in Table 2.1.

Table 2.1. The recent status of critical current density (J_c) of MgB₂

4.2 K					
Type	Sheath material / Substrate	J_c at 8 T (A/cm²)	J_c at 6 T (A/cm²)	J_c at 2 T (A/cm²)	Reference
WIRE	Ta, Cu			2×10^4	(Canfield et al. 2001)
	Cu		10^4	6×10^4	(Eisterer et al. 2002)
	SS		2×10^4	10^5	(Serquis et al. 2003)
	Fe		2×10^4	10^5	(Dou et al. 2002)
FILM	Al ₂ O ₃	5×10^4	10^5	2×10^6	(Bu et al. 2002)
	SrTiO ₃	1.6×10^5	2.7×10^5	8×10^5	(Eom et al. 2001)
	YSZ	10^5	2×10^5	2×10^5	(Komori et al. 2002)
BULK	-	10^2	6×10^2	10^4	(Flukiger et al. 2003)
	-		10^2	5×10^4	(Wang et al. 2002)
20 K					
Type	Sheath material / Substrate	J_c at 4 T (A/cm)	J_c at 2 T (A/cm)	J_c at 0 T (A/cm)	Reference
WIRE	Fe	2×10^3	5×10^4	5×10^5	(Suo et al. 2002)
	Ta			2×10^5	(Canfield et al. 2001)
	SS		10^5		(Giunchi et al. 2002)
FILM	Al ₂ O ₃		4×10^4	2×10^6	(Pradhan et al. 2001)
	SrTiO ₃		1.7×10^5	2×10^6	(Eom et al. 2001)
	Al ₂ O ₃			7×10^6	(Moon et al. 2001)
BULK	-	5×10^3	3×10^4	7×10^5	(Kim et al. 2002)
	-	10^3	7×10^3	8×10^4	(Zhao et al. 2002a)

There are two other superconductor materials that are comparative to MgB₂ as was mentioned before. These materials are NbTi and Nb₃Sn. Their critical current density values at zero field, and 8 Tesla are 10⁷ A/cm², 8 × 10⁴ A/cm² and 10⁷ A/cm², 10⁵ A/cm² respectively at 4.2 K. It can clearly be seen from the Table 2.1, that for MgB₂ wires and bulk samples critical current density values are less than the values of conventionally used superconductors (at 4.2 K).

Researchers have focused on the chemistry and stoichiometry variation of MgB₂. They introduced various additive elements or substitutions on the Mg or on the B side of MgB₂ and studied the field and temperature dependence of the critical current density (J_c). Studies were on bulk MgB₂ samples with the elements, Li, Na, Ca, Ag, Cu, Al, Zn, Zr, Ti, Mn, Fe, Co and C. Yet, so far only Al has been found to really substitute for Mg yielding a solid solution with gradually decreasing transition temperature (T_c). A decrease in transition temperature has been observed for all the additives, but among all additives mentioned above Ti, Zr₂O and SiC provides an improvement on the critical current density values in zero field and especially in magnetic field. Zhao et al. reported an increase of J_c after doping with Ti and Zr, which was interpreted as a result of nanosize defects at grain boundaries of MgB₂ (Zhao et al. 2002a, Zhao et al. 2002b, Feng et al. 2001). In type II superconductors, creating more pinning centers in the superconductor improves the J_c of the material. Therefore in Ti addition case, although Ti does not occupy an atomic site in the MgB₂ and the TiB₂ phase grows at the grain boundaries of MgB₂ in nano size and behaves as pinning centers. Thus increases the critical current density. List of the additives, which has a positive improvement on the superconducting properties of MgB₂ are summarized in Table 2.2.

Table 2.2. Effects of additives on J_c of MgB₂ at 20 K.

20 K					
Type	Additive	J_c at 4 T (A/cm²)	J_c at 2 T (A/cm²)	J_c at 0 T (A/cm²)	Reference
BULK		2 × 10 ³	3 × 10 ⁴	5 × 10 ⁵	(Canfield et al. 2001)
	Ti	10 ⁴	10 ⁵	10 ⁶	(Zhao et al. 2002a)
	Y ₂ O ₃	5 × 10 ³	8 × 10 ⁴	3.5 × 10 ⁵	(Flukiger et al. 2003)
	SiC	3 × 10 ⁴	2 × 10 ⁵	6 × 10 ⁵	(Flukiger et al. 2003)

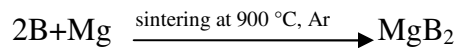
In this study Mg addition is applied to some wires. The reason for choosing, Mg is that, it was found that unreacted Mg improves the critical field and critical current density of the MgB₂ and also studies on the substitutional chemistry of MgB₂ indicated the inertness of Mg to MgB₂ even if at high temperatures. In literature, Jung et al. studied the effects of unreacted Mg on the normal state and superconducting properties of MgB₂ intensively (Jung et al. 2002).

Addition to critical current density, critical fields (upper critical field, H_{c2} and irreversibility field, H_{irr}) of the superconductors are significant parameters when the application point of view is considered. The upper critical field of MgB₂ is anisotropic because of its layered structure. Recent measurements of H_{c2} on single crystals indicates that the H_{c2} parallel to the c axis is low about 3 to 4 Tesla at T=0 K. The H_{c2} value for H parallel to the ab plane is about 15-20 Tesla at T=0 K. The resultant anisotropy is (the ratio of the value parallel to ab plane to c plane) is ~4 (Buzea and Yamashita 2001). The calculated values of the GL coherence length of the MgB₂ is ξ_{ab} = 5-8 nm and ξ_c = 2-3 nm. The mean free path (l_{ab}) of MgB₂ single crystals is as large as 50-100 nm (Canfield et al. 2001), which reveals that MgB₂ is in the safe side ($l_{ab}/\xi_{ab} \gg 1$). Then again, in terms of applications the value of irreversibility field is more important than upper critical fields of superconductors because the applications are limited by the irreversibility field. The value of irreversibility field for MgB₂ is about 8-12 Tesla for single crystals. The upper critical field and the irreversibility field strengths of MgB₂ are poor for applications, compared with Nb based superconductors. However the artificial introduction of impurities or defects may lead to reduction in ξ , and therefore an increase in H_{c2} by the Ginzburg-Landau-Abrikosov-Gorkov (GLAG) impurity effect. For instance for Fe clad wires an upper critical field of 28 T was reported by Flukiger et al (Flukiger et al. 2003). Existence of anisotropic nature is also observed in the lower critical field (H_{c1}) of MgB₂. The H_{c1} value parallel to c axis is 27.2 mT at T=0 K. The H_{c1} value parallel to ab axis is 38.4 mT at T=0 K (Xu et al. 2001). From the polycrystalline data for H_{c1}, the magnetic penetration depth can be roughly estimated as $\lambda(0) \sim 170$ nm using $H_{c1} = \phi_0 \ln \kappa / (2\pi\lambda^2)$.

2.3 Preparation of Bulk Samples from MgB₂

2.3.1 Synthesis of MgB₂

Even though there are several methods to prepare MgB₂ they all have the same basis of a solid-state reaction between Mg and B atoms. The stoichiometric mixture of Mg and B (Mg + 2B) is annealed at 900°C for 2 hours in argon atmosphere, especially in a sealed tube as Mg is an extremely volatile element.



There are many factors effecting the quality and cost of the resultant MgB₂. The approach followed in production and the quality of initial Mg and B are two of these elements. To obtain MgB₂ by solid state reaction, initial stoichiometry of Mg and B is not significant. When the usage in applications is considered, the quality of the obtained powder is essential. Hinks et al. studied the effects of stoichiometric variation on the sintering of MgB₂ (Hinks et al. 2002). In this study Hinks studied the excess Mg and deficient Mg in Mg_xB₂, for varying concentrations of x. (0.5 ≤ x ≤ 1.3) MgB₂ phase is observed also for x = 0.5 and x = 1.3 conditions. Beginning composition ratio is a factor altering the superconducting properties. Also the purity of final MgB₂ is dependent on the purity of initial Mg and B, and purity is found to be affecting more on the superconducting properties of MgB₂ than the stoichiometric composition does. One of the major factors affecting the residual resistivity ratio (RRR = ρ(300K)/ρ(40K)) of MgB₂ is the purity of B powder (Riberio et al 2002, Gunel 2003). A related study was carried on by Ribeiro et al. and formation of MgB₄ phase in the Mg deficient samples was announced (Ribeiro et al. 2002a). Both Hinks and Ribeiro observed the highest transition temperature in stoichiometric samples for x=1, for Mg_xB₂. In addition a decreasing residual resistivity ratio (RRR) is observed for Mg poor samples. An increasing RRR is observed in samples with excess Mg for all cases. Unlike Hinks, Ribeiro the effects of boron purity on the sample quality and the RRR of the samples were studied. A higher RRR and lower resistivity 0.4 μ Ωcm was observed in the samples that have highest Boron purity.

It is difficult to obtain dense MgB₂ bulk samples because MgB₂ has very low fracture toughness. The theoretical density of MgB₂ is 2.62g/cm³. There are numerous methods to obtain dense MgB₂ bulk samples. High density MgB₂ samples were prepared using hot isostatic pressing technique. In this study, the densities on the average 2.3g/cm³ were obtained which were very close to theoretical density of MgB₂ (Serquis et al. 2003).

2.3.2 Metal Matrix Composite (MMC) Method

MgB₂ is difficult to use in bulk applications due to its brittleness. There are two solutions to this problem. The first one is cladding of MgB₂ wires or tapes with a ductile metallic sheath and an alternative approach is to create a metal matrix composite (MMC) consisting of a small scale, isotropic mixture between superconducting MgB₂ phase and a ductile metallic phase. The advantage of using MMC method is that the metal improves fracture toughness, ductility and crack arrest, and also acts as a heat and electric conductor in case of localized breakdown in superconductivity in the MgB₂ phase. The particulate constituent increases the hardness and elastic modulus. While the MMC approach is widely used for brittle ceramic cuprate and intermetallic Ni-based superconductors (with Ag and Cu matrices, respectively), there are only two articles on MgB₂ based metal matrix composites. In the first study Ti powders were mechanically alloyed with 4 wt % MgB₂ powders at room temperature and they were found to react at 600°C to form a ternary boride which is not superconducting. In the other study, a compacted mixture of MgB₂-11 wt % Al powders was vacuum sintered 317°C into a composite exhibiting superconductivity at 38 K.

MMC method is a new method for superconductors. The two ways of obtaining MMCs are liquid infiltration and hot pressing techniques. Liquid-metal infiltration is a method where a ceramic perform (consisting of packed powders, whiskers or fibers) is infiltrated usually under pressure to overcome capillary forces, by a metallic melt which is subsequently solidified is the commonly used method to prepare MMCs. Dunand and Giunchi et al. obtained MgB₂ metal matrix composites with liquid infiltration method with Mg metal phase (Dunand 2001, Giunchi et al. 2002). Dunand used both traditional infiltration method (commercial MgB₂ and liquid Mg) and reactive infiltration method (B powders and liquid Mg) following a heat treatment. In this study MgB₂/Mg

composites produced liquid infiltration of Mg into MgB_2 were observed to have a density about 2.07g/cm^3 and a transition temperature of 38 K. However MgB_2/Mg composites produced by liquid infiltration of Mg into B powders were observed to be very brittle after heat treatment and have critical temperature below 37 K (Dunand 2001). As mentioned above MMC method is new method for superconductors and there are a few studies about this method only used with liquid infiltration. Although there are not many studies about preparing MMCs by hot pressing technique, there is one study by (Egilmez et al. 2004), where Mg/MgB_2 MMCs were produced by hot pressing technique.

2.3.3 Powder In Tube (PIT) Method

Powder In Tube method (PIT) is a very convenient way of fabricating MgB_2 tapes and wires of industrial lengths. The PIT process is very beneficial because of low material costs and relatively simple deformation techniques. Moreover it is the only way of producing multi filamentary wires and tapes. Multi filamentary wires withstand larger uniaxial and bending strains than single filaments as known from the Nb_3Sn and Bi-2223 wires. And they exhibit a higher thermal stability due to the smaller cross section of the individual filaments. PIT method has been extensively used for both conventional and high temperature superconductors. In this method brittle superconducting powder is filled into a ductile metal tube and than swaged into small diameters for various applications. The schematic representation of PIT method used with Fe metal sheath is seen in Figure 2.4.

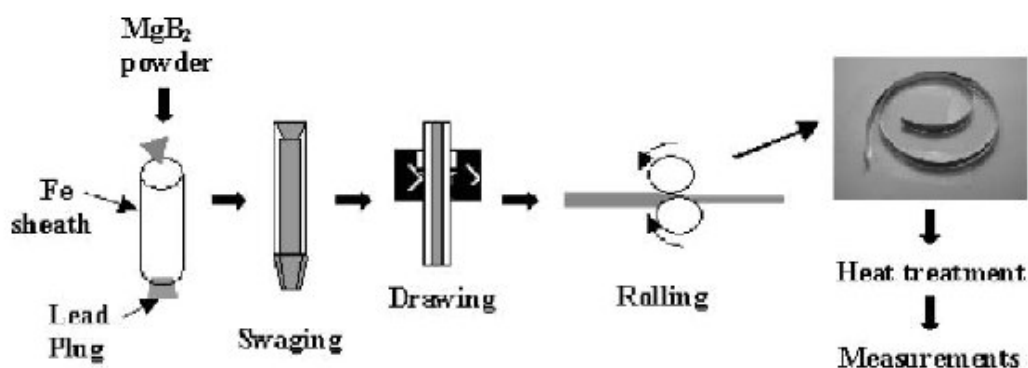


Figure 2.4. Schematic representation of Powder In Tube Method

Recently, there are many research groups which have successfully produced wires and tapes with PIT method, either with or without an application of a heat treatment (Xiao et al. 2003, Glowacki et al. 2001, Goldacker and Schlachter 2002, Kamakura et al. 2001). There are critical points to be careful about while PIT method is used. These are maintaining critical temperature (T_c) and critical current density (J_c) while improving mechanical properties of the superconductor during the mechanical deformation or following annealing process. Then again, a possible reaction between metal and superconducting phase may degrade the superconducting properties of the wire. Consequently, substitutional chemistry of the superconducting material is significant. Thus, various metal sheaths such as stainless steel SS (Kamakura et al. 2001), Cu (Glowacki et al. 2001), Ag (Glowacki et al. 2001), Cu-Ni (Kamakura et al. 2001), and Fe (Soltanian et al. 2001, Feng et al. 2003) has been used to produce metal/MgB₂ composite wires with PIT method. Owing to its high critical current density of $1.42 \times 10^5 \text{ A cm}^{-2}$ (4.2 K, 4T) and its inertness to MgB₂ even with annealing at 900°C (Feng et al. 2003), iron was determined to be the best sheath material for MgB₂ wires.

In Figure 2.5 SEM macrographs of the cross section of a monofilamentary Fe clad MgB₂ tape is observed. In Figure 2.5(a) and 2.5(b) the transverse and longitudinal cross section of a deformed Fe/MgB₂ are seen to be quite uniform. The comparison of SEM pictures of a polished crossed section of MgB₂ core after deformation (Figure 2.5(c)) and after annealing at 950°C for 30 minutes (Figure 2.5(d)) clearly shows the densification during the heat treatment. In PIT, heat treatment enhances fill factor by

densification. As a result, the fill factor of the tape which is a crucial parameter when carrying high critical currents is in demand is improved.

Furthermore, there is another advantage of heat treatment. It may also lead to an oxidation in the superconducting core which later acts as pinning centers. This is also observed in the Fe clad tapes mentioned above as the XRD results showed an increase in the amount of MgO. This amount of MgO in MgB₂ behaves as pinning centers and improves the critical current density of the tape (Feng et al. 2003).

Until now the examples of PIT method given above, are tapes and wires prepared by exsitu preparation. On the other hand PIT method can also be used with insitu preparation. In insitu preparation method, Mg powder and B powder are filled into a metal sheath and then annealed. A benefit of using insitu preparation technique is that new pinning centers can be introduced to the material in addition to the existing intrinsic pinning centers of MgO, by doping with different elements like Ti (Zhao et al. 2002a, Zhao et al. 2002b, Feng et al. 2001).

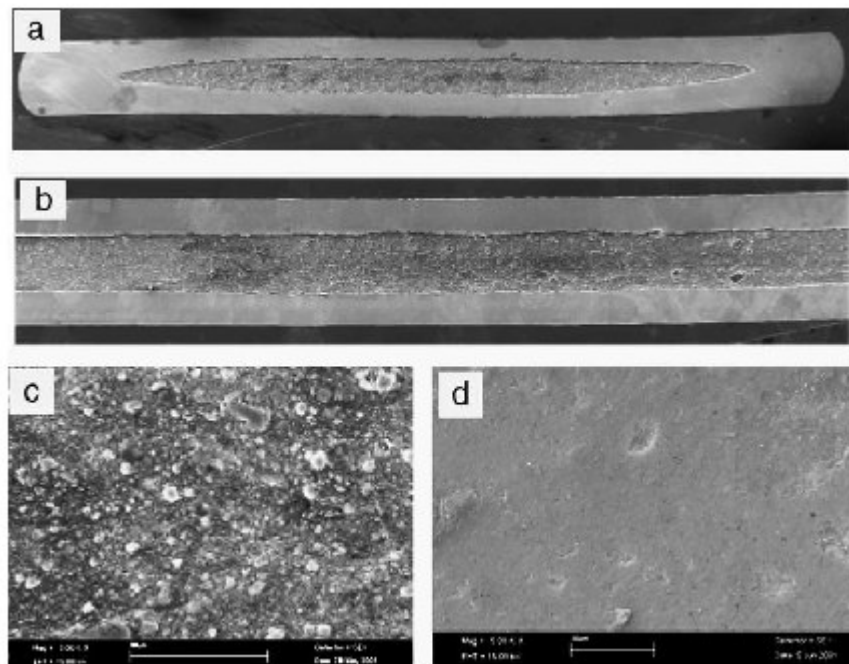


Figure 2.5. SEM Images of Fe clad tapes a) Transverse b) Longitudinal c) After Deformation d) After Annealing.

CHAPTER 3

EXPERIMENTAL METHODS

3.1 Material Preparation

3.1.1 MgB₂ Synthesis

MgB₂, as mentioned in the previous chapters, draws great attention as a new material for applications based on superconductivity. Therefore one of the most important aspects of this thesis is to be able to produce MgB₂. For this purpose, initially B synthesis is required. After B is synthesized, it needs to be purified through several acid leaching steps. The reason why synthesized B is not fully ready to be used in the MgB₂ production yet, is that it contains a major impurity of MgO. To be able to remove MgO, acid leaching steps using Hydrochloric acid (HCl) is applied. Commercial Mg (99.9999 % purity, 31-44 μm average particle size, Alfa Aesar) is the other element to be used in MgB₂ synthesis. Finally, successful synthesis of B powder and usage of commercial Mg powder leads to synthesis of MgB₂. Synthesis processes followed in this study will be given in more detail in the following parts.

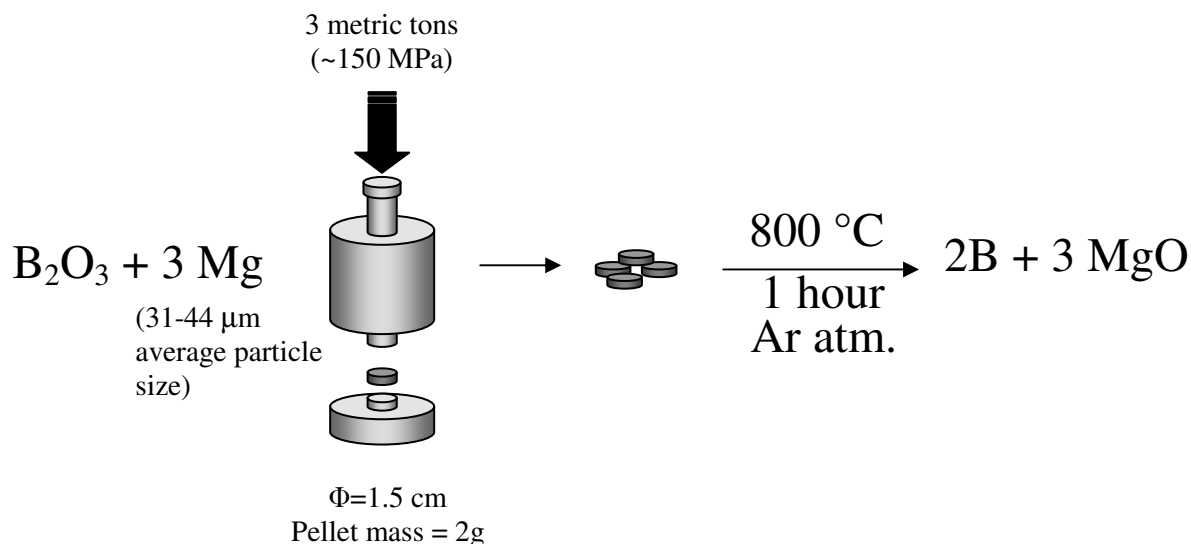


Figure 3.1. A representation of the solid state reaction to produce elementary B powder.

Keeping in mind the fact that Turkey is rich in boron oxide (B_2O_3), the elementary B used in this study is meant to be synthesized from B_2O_3 . B_2O_3 (98.5 %) provided from ETİ BOR and commercial Mg (Alfa Aesar) were mixed in stoichiometric ratio and pressed to pellets of 2g under 150 MPa of pressure. The pellets are subjected to solid state reaction at 800°C in Ar atmosphere for 1 hour. The particle size of the resulting powder at the end of this solid state reaction is reduced in a mortar.

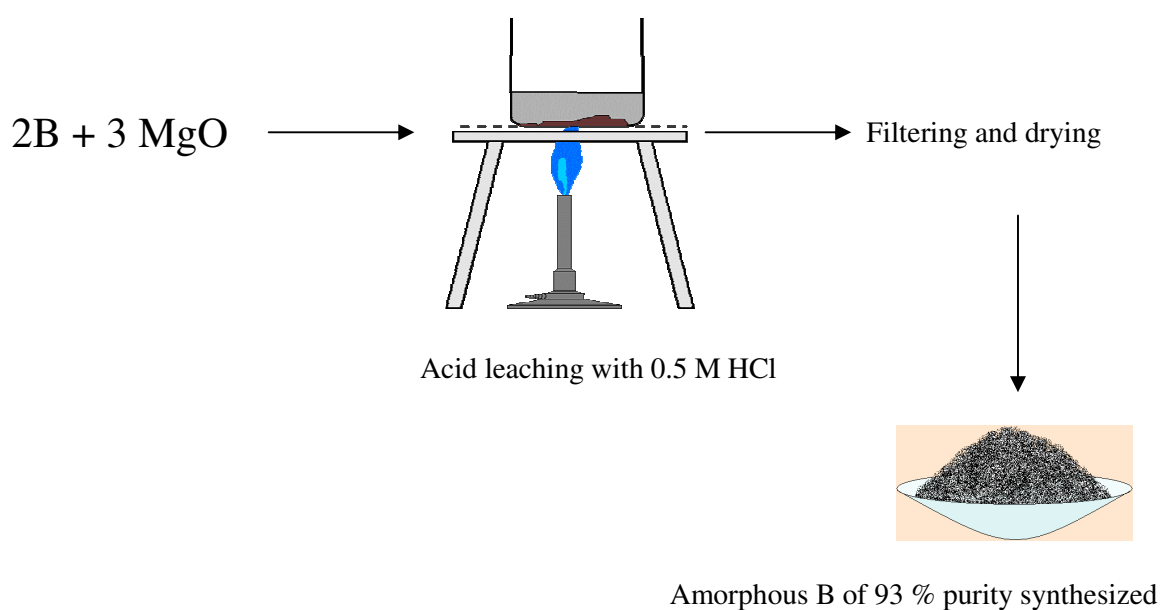


Figure 3.2. Purification process of B powder through Acid Leaching by HCl.

XRD measurements of the powder revealed that this resulting powder consists of MgO and B. To remove MgO, acid leaching with 0.5 M Hydrochloric acid (HCl) was applied to powder, which contains elementary B and MgO. High purity (93.05 %) B was obtained after a repetitive process of acid leaching.

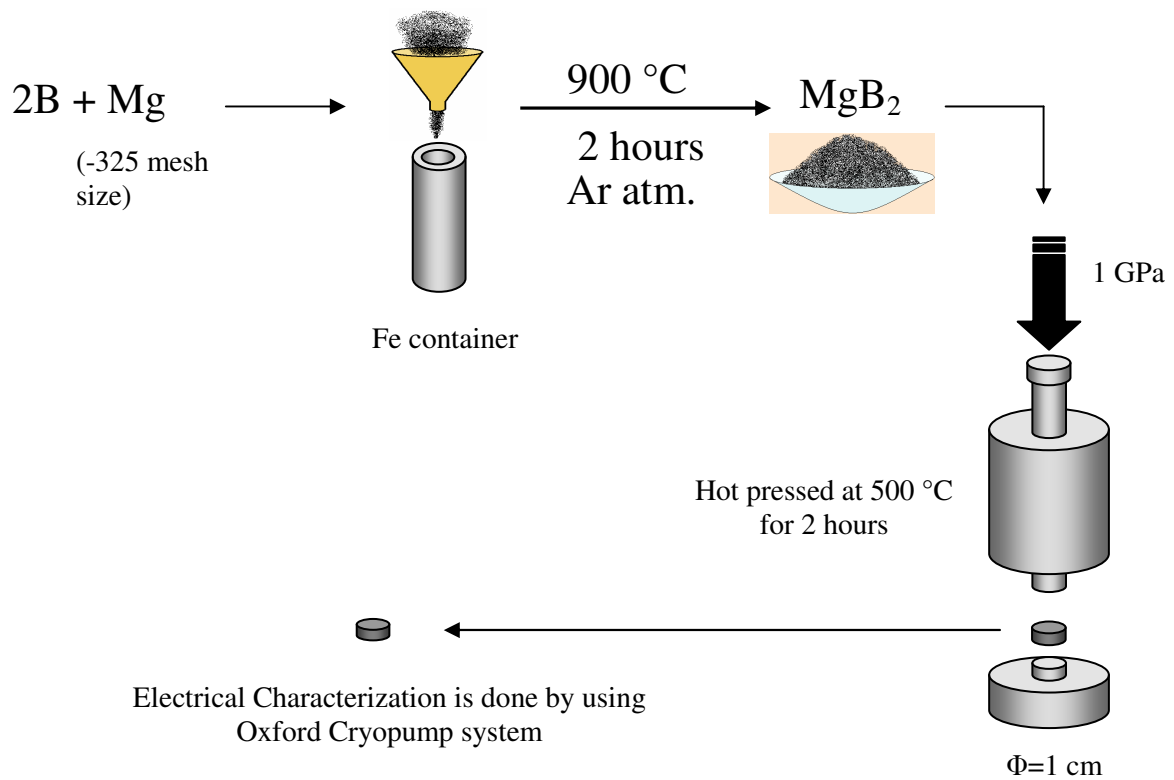


Figure 3.3. MgB₂ pellet production.

Produced elementary B and Mg were mixed in stoichiometric ratio and filled in a Fe container and subjected to solid state reaction in Ar atmosphere at 900°C for 2 hours. Produced MgB₂ powders were hot pressed in a cylindrical metal die at 500°C for 2 hours to pellet of diameter of 1cm, under a pressure of 1GPa.

3.1.2 Pellet Production

Commercial MgB_2 powder (Alfa Aesar) and C powders were used for the fabrication of MgB_2/C composites. The weight ratio of C to MgB_2 was 0%, 1%, 2%, and 3% for different set of samples; MgB_2 and C powders were mixed homogeneously and uniaxially pressed under pressure of 1 GPa in a metallic die. The die was heated to 500°C and kept at this temperature for 2 hours in air as shown in Figure 3.3, the temperature was controlled with a variac and a thermocouple connected to Omega temperature controller.

For electrical, microstructural characterization, fabricated pellets were about 1.1 mm in height and 10 mm diameter. During electrical characterization, four point probe resistivity measurement was done for 0.1 mA, 0.5 mA, 1 mA, 2 mA, 3 mA, and 5mA current values. Temperature dependence of both normalized resistance and resistivity graphs were plotted.

3.1.3 Powder in Tube Method (PIT)

Many applications of superconductors require coils to produce high magnetic fields and in order to produce coils, long lengths of wires are necessary. One of the most conventional ways of MgB_2 wire production is Powder In Tube (PIT) method. The popularity of this method is due to low material costs and simple deformation techniques. What is more, it is the only way of producing multi filamentary wires and tapes. MgB_2 is a very brittle material and it needs cladding by a more ductile material to be suitable for wire production. Therefore in this study the PIT method is used to prepare Cu clad wires of MgB_2 .

The preparation process consists of several steps. In the first step, MgB_2 powders of -325 mesh size were filled in Cu tubes of 1 mm wall thickness and 5mm outer diameter (Figure 3.4a)

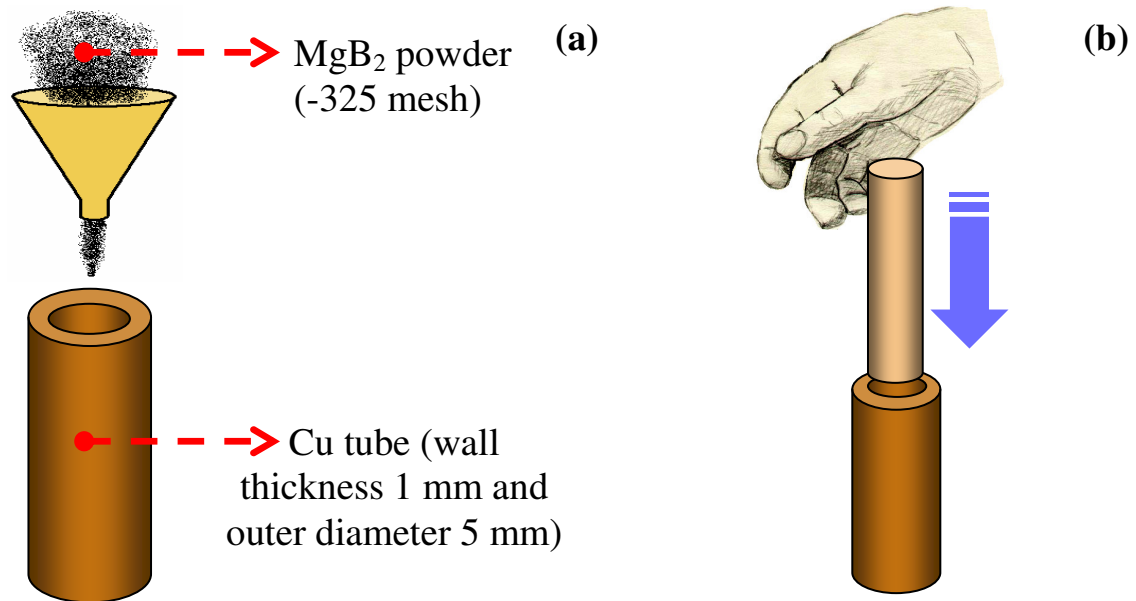


Figure 3.4a. Representation of filling Cu tube with MgB₂ powder
 Figure 3.4b. Representation of hand pressing of MgB₂ powder

Then, as the resultant pellets are desired to be as dense as possible, hand pressing was applied to densify the MgB₂ powder inside the Cu clad (Figure 3.4b).

Next step is to reduce the wire diameter which results in a natural increase in the wire length. The wire is swaged to smaller diameters to the desired thickness. This process is called cold drawing. After each step there is about 5% section reduction.

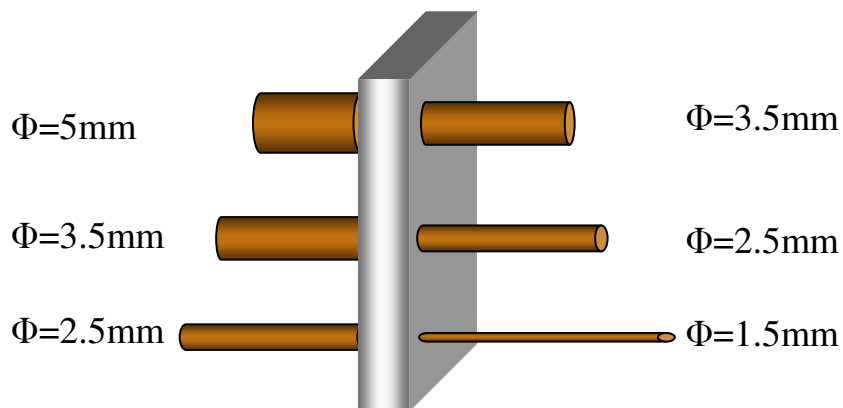


Figure 3.5. Cold drawing Process

Superconducting fill factor corresponds to about 25% - 30% for the whole conductor volume.

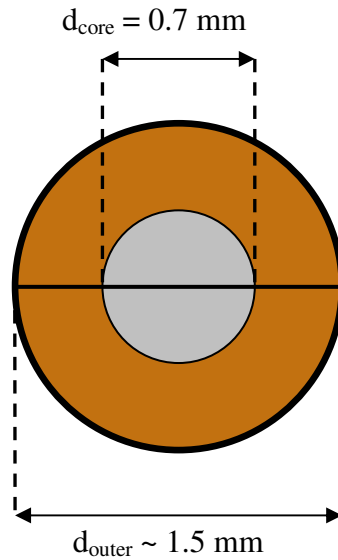


Figure 3.6. Cross-sectional view of Cu clad MgB₂ wire.

The prepared samples were then annealed in a tube furnace in an Ar gas flow under ambient pressure under various temperatures to see the effect of annealing for some samples.

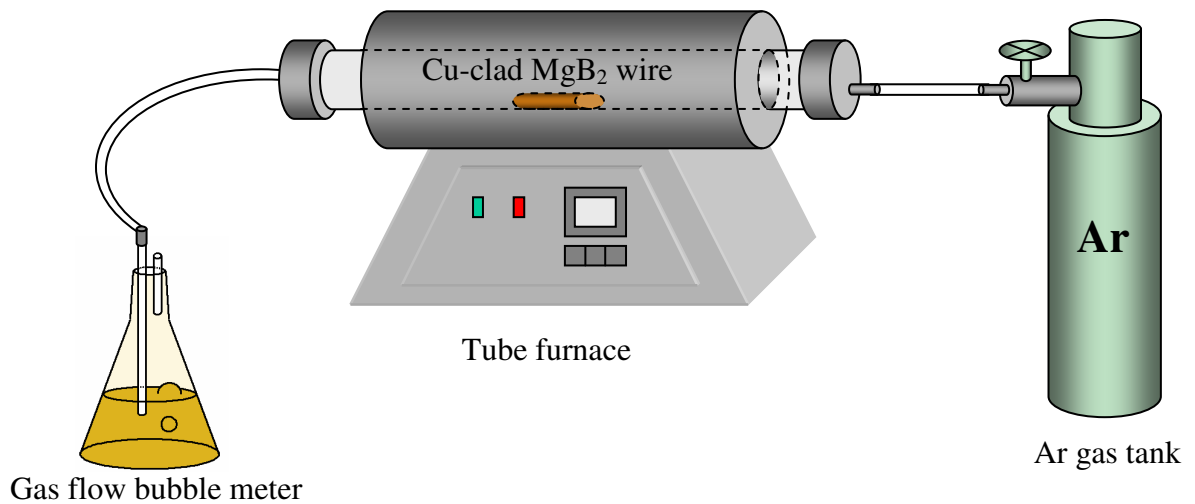


Figure 3.7. Annealing System

3.2 Characterization Methods

3.2.1 Four Point Probe Method

The DC resistivity of a sample is measured by the voltage drop across a specimen when a current of known magnitude passes.

The most accurate approach to measure T_c is at low fields and low currents, since the transition temperature of a superconductor depends on both applied field and applied current. The measurement can be done for example by applying 0.1 mA. When a high impedance voltmeter is connected to the terminals used for measuring the voltage, only a little current is allowed to pass through. These terminals are distinct from those used for passing the main part of the current through the specimen, where voltage drops in both leads and contacts are significant. Figure 3.8 shows a schematic diagram of four probes connected to a sample whose temperature is measured by temperature sensor close to the specimen and similarly well connected on the surface of cold head.

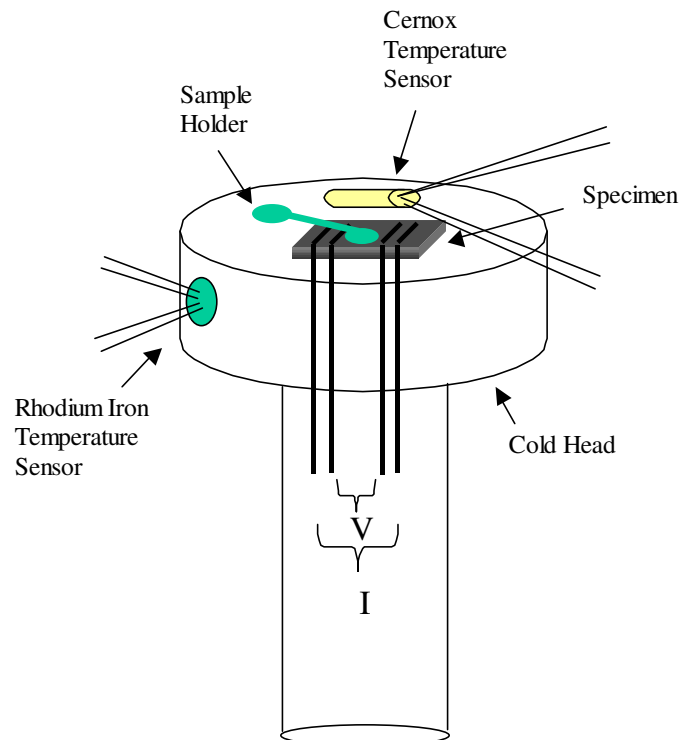


Figure 3.8. Four Probe Method

In order the thermal contact between the specimen and the surface of the cold head to be well established, it is significant to use thermal conductive grease between the specimen and the surface.

During four point resistance measurements the contacts on the specimen is used to minimize the effects of lead resistance mainly in low resistance measurements. Moreover, additional corrections can be made for thermal emf's by reversing the current at each reading and taking the average voltage generated across the specimen for the two direction of current flow. The measurements were carried on with a computer controlled Cryo system, Figure 3.9. This system provides us to have the temperature dependence of samples between 20 K and room temperature. The system consists of an Oxford Edward Cryostat 1.5, Coolstar cold head model 2/9, Keithley 220 current source, Keithley 2582 nanovoltmeter, Edward mechanical pump, ITC 502 temperature controller GPIB connectors and IEEE 488.2 interface cards for the connection to the computers. The data acquisition software was written in Objectbench. The corrections for thermal emf's by reversing the current at each reading was done by the software.

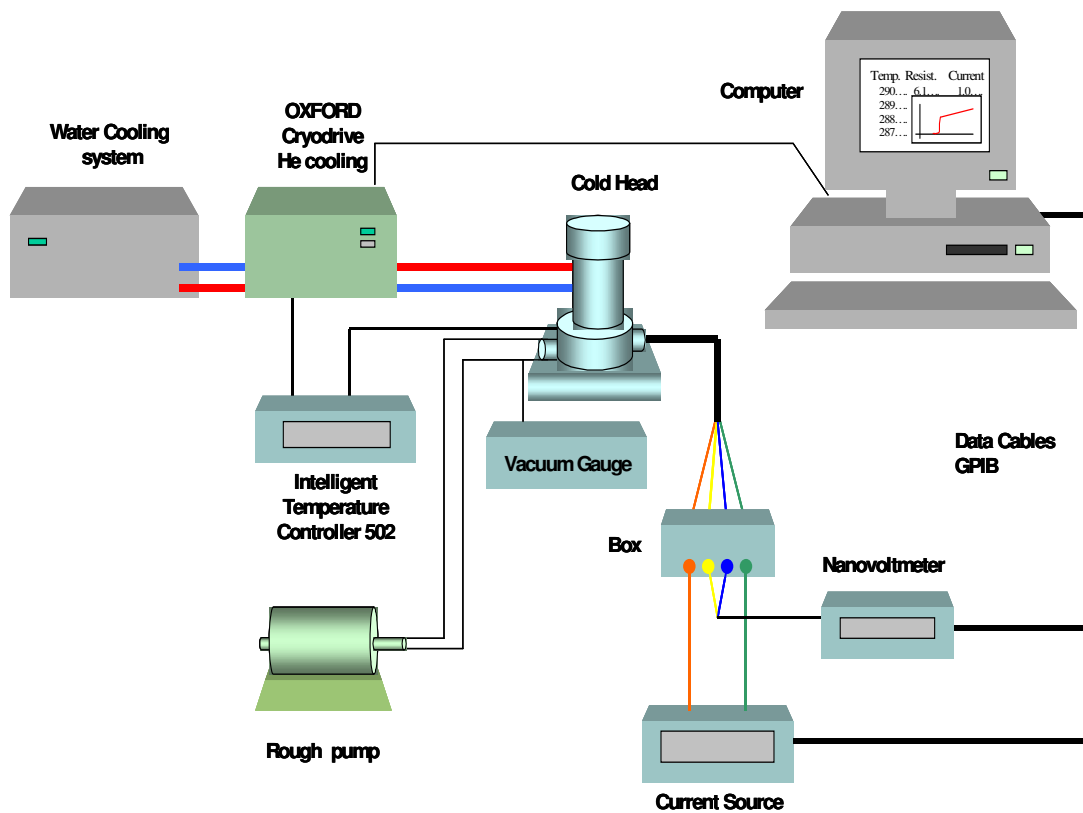


Figure 3.9. Closed Cycle Cryopump System

In order to understand the superconducting and microstructural properties of obtained superconductive powder pellets and wires many characterization methods are applied. XRD, SEM and EDX techniques were used for the microstructural analysis and phase determination. Closed-cycle cryopump system for the electrical properties and resistivity measurements of rectangular pellet samples and wires were analyzed.

CHAPTER 4

RESULTS AND DISCUSSIONS

In the first part of this thesis, elementary B synthesis, purification of this B, MgB₂ synthesis and microstructural and electrical characterization of the pellet produced from synthesized MgB₂ is aimed. In the second part, C added MgB₂ pellet production by MMC method is studied. Temperature dependence of resistance of C added MgB₂ pellets are investigated. In the third part, Cu sheath Mg added MgB₂ wires are produced by PIT method and electrical and microstructural characterization of these wires are done through XRD, SEM, EDX and R-T measurements.

4.1 Elementary B and MgB₂ Synthesis Results

4.1.1 Elementary B Synthesis Results

In this thesis, firstly MgB₂ synthesis is investigated. For this aim, elementary B production is taken to be the primary step. The importance of B for the MgB₂ production is evident, but purpose of our study is also supported by the fact that Turkey is very rich in B. The elementary B powders have been submitted to several acid leaching steps to ensure purification. To show the effect of purification process, weight percentage versus acid leaching steps is examined.

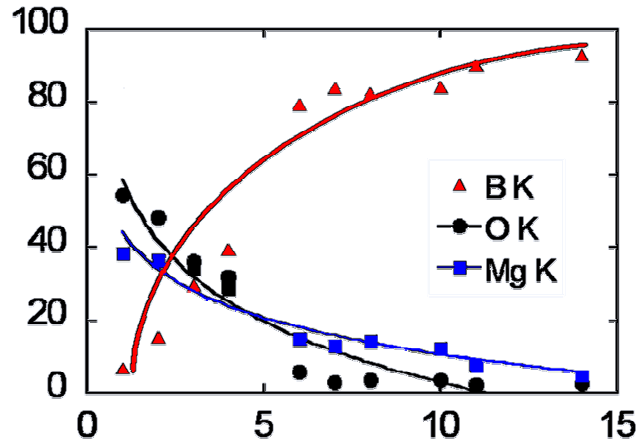


Figure 4.1. Variation of produced B purity with respect to acid leaching steps.

Table 4.1. Weight percentage of the elements before and after acid leaching.

Before Acid Leaching		After Acid Leaching	
Element	Weight Percentage	Element	Weight Percentage
B K	6.97	B K	93.05
O K	54.47	O K	2.57
Mg K	38.56	Mg K	4.38

EDX analysis was carried out in order to detect Boron amount and purity in the produced amorphous powder. After repeating acid leaching process, EDX analysis of the produced powder given in Figure 4.1 shows that its purity is 93.5 % and Mg impurity is around 5 %. 5% Mg impurity in the amorphous Boron powder is not important, since the final goal is to obtain superconducting MgB_2 using another solid-state reaction of produced amorphous B powder with high purity commercial Mg. Reducing the amount of Mg by 5% in the solid-state reaction to obtain superconducting MgB_2 powder compensates this impurity of the B. The purity of obtained Boron increases with increasing number of acid leaching steps as shown in EDX analysis (Figure 4.1). Repeating the acid leaching steps has an important role in Boron purity. The ratio of Boron in the initial output product is 6.97 %. Then it increases to 16 % after

first acid leaching and it is above 80 % after 6th step. Finally, after 13th step, 93% of amorphous elementary B purity was reached.

XRD patterns of the 2B+MgO powders after the reaction of B₂O₃ and Mg at 800°C for 1 h in Ar atmosphere before and after acid leaching is shown in Figure 4.2. The peaks before acid leaching were changed into a noise showing only amorphous B after acid leaching process. This case shows all the phases except MgO and B in the sediment disappeared.

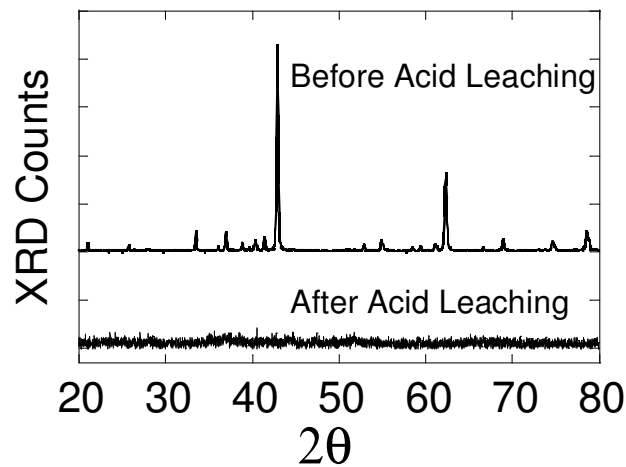


Figure 4.2. XRD patterns of the powders before and after acid leaching of the powders obtained after the reaction of B₂O₃ and Mg at 800°C.

After acid leaching the XRD results also show that the MgO phase has disappeared.

4.1.2 MgB₂ Synthesis Results

The next step is to mix the produced B powder with commercial Mg powder in stoichiometric ratios to prepare MgB₂. To see the suitability of the synthesized MgB₂ to applications, a pellet using this MgB₂ is prepared. The XRD, SEM, and R-T measurements of this sample will be discussed in detail below.

For the production of MgB₂, elementary B is reacted with pure Mg of -325mesh at 900°C in Ar atmosphere for 2 hours. Since Mg vaporizes in the production

temperature of MgB_2 , mixing Mg and B in a stoichiometric ratio causes the amount of Mg in produced MgB_2 to be less than its stoichiometric value. This non-stoichiometry situation may degrade the superconducting properties. For this reason 10% of excess Mg is added to conserve the stoichiometry after the reaction.

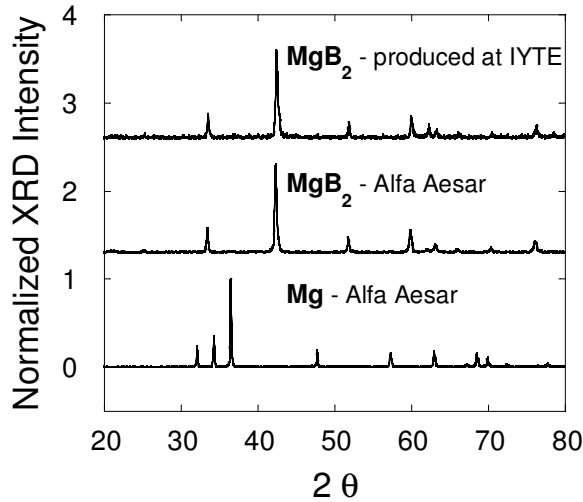


Figure 4.3. XRD patterns of the produced MgB_2 .

XRD results of MgB_2 powder obtained from the reaction of produced elementary B and Mg at 900°C in Ar and commercial Mg and MgB_2 is given in Figure 4.3.

The produced and commercial MgB_2 peaks matches exactly except a Mg peak present at $2\theta = 63.6$ as impurity.

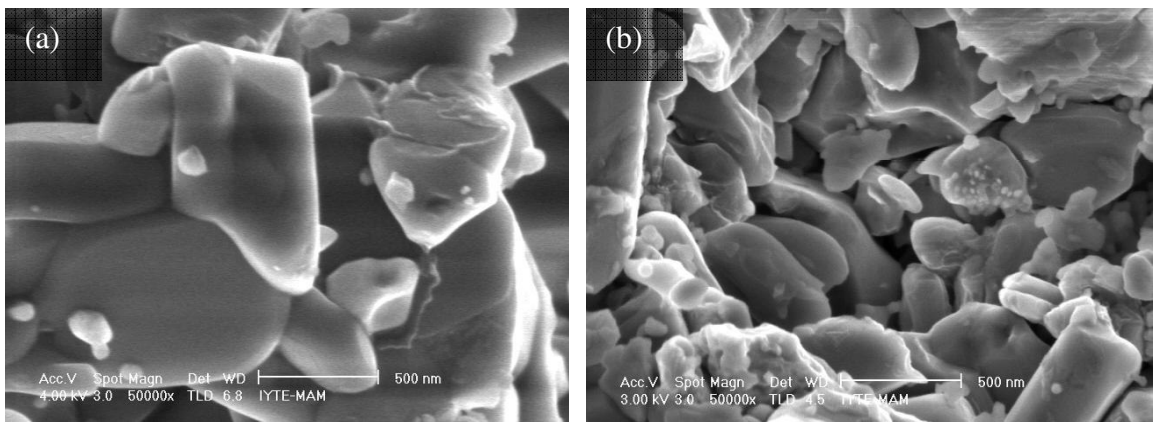


Figure 4.4a. SEM image of produced MgB_2 as powder
Figure 4.4b. SEM image of produced MgB_2 as pellet

SEM images of produced MgB_2 in powder form and in a pellet compressed at 1 GPa at 500°C for 2 hours are shown in Figs. 4.4a and 4.4b respectively. The average particle size is smaller for the pellet comparing with powder form due to pressure and annealing. Small particle size increases grain boundary to increase critical current density. This is also important superconducting parameter of the material to improve pinning properties (Zhao et al. 2002a).

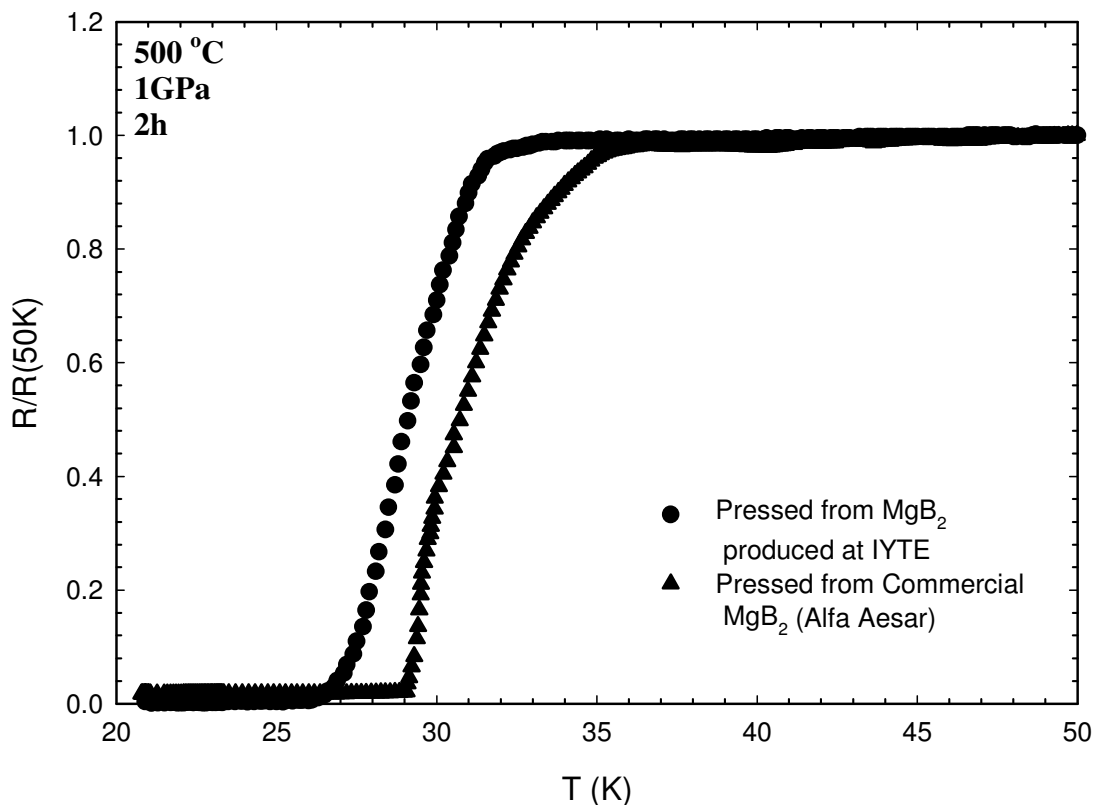


Figure 4.5. Temperature vs. Resistance plots of pellet pressed from MgB_2 produced at IYTE and pellet pressed from commercial MgB_2 (Alfa Aesar).

Rectangular samples cut out from the pellets to measure the temperature dependent resistivity between 300 K and 20 K. Normalized resistance versus temperature plot for fabricated MgB_2 starting from B_2O_3 is given in Figure 4.5. The produced superconducting MgB_2 pellet makes a transition at 32 K. It is measured that the density of the superconducting MgB_2 pellet was 1.99 g/cm^3 . This value is smaller than the theoretical value of MgB_2 of 2.62 g/cm^3 . This shows that there is large amount

of voids present in the material. This high porosity ratio causes low grain connectivity between MgB_2 grains. The low transition temperature and broaden transition interval indicate low grain connectivity due to porosity in the material.

The XRD, EDX, SEM and temperature dependence of resistivity results revealed that superconducting MgB_2 is successfully produced from the reaction of Mg and B reduced from the B_2O_3 . DC resistivity measurement was done to determine the superconducting properties of the produced powders. The produced superconducting MgB_2 pellet shows a T_c onset value of 32 K. There is a slight difference between T_c values of the pellet pressed from MgB_2 produced at IYTE, and the pellet pressed from commercial MgB_2 . This difference which can be seen in Figure 4.5, is considered to be a result of impurities left in the material in the purification process of B.

4.2 C Added MgB_2 Pellet Production Results

In this study, different than what has mostly been practiced in literature, C is not doped or substituted to one of the constituents of MgB_2 , but added to it. Commercial MgB_2 powder (Alfa Aesar) and C powders were used for the fabrication of MgB_2/C composites. The weight ratio of C to MgB_2 was 0%, 1%, 2%, and 3% for different set of samples; MgB_2 and C powders were mixed homogenously and uniaxially pressed under pressure of 1 GPa in a metallic dye. The dye was heated to 500°C and kept at this temperature for 2 hours in air.

Densities of the pellets are in Table 4.2. These values obtained, were very close to theoretical density of MgB_2 which is 2.62g/cm^3 (Serquis et al. 2003). This difference indicates that produced pellets have porosity.

Table 4.2. Densities of the pellets with 0%, 1%, 2% and 3% C addition to MgB_2

	0% C	1% C	2% C	%3 C
Densities (g/cm^3)	2.29	2.30	2.30	2.29

The effect of C doping or substitution is found to be a decrease in the critical temperature of the samples but on the other hand an enhancement is observed in the

magnetic properties of the specimen. However in this study, a new approach C addition is applied to see the effect on T_c . The electrical characterization results will be presented with temperature dependence of resistance plots (Ribeiro et al. 2002b, Paranthaman et al. 2001, Bharathi et al. 2002).

Temperature dependence of resistance can be seen from the figures 1,2,3,4 for 0%, 1%, 2%, and 3% C added pellets respectively. The pellets were hot pressed at 500 °C at 1GPa for two hours. For each graph resistance versus temperature data was collected by deriving current values of 0.1 mA, 0.5 mA, 1 mA, 2 mA, 3 mA, 5 mA, and 10 mA to the system. A closer and careful look at the plots reveal that as the deriving currents increase, the measurement becomes more reliable with less noise in data. But as expected, effect of joule heating can be seen, as the deriving current increases, T_c for the entire set of samples, shift to higher values. For 0%, 1%, 2%, and 3% C added pellets, the transition temperatures can be seen from Table 4.3.

Table 4.3. Transition temperatures of the pellets with 0%, 1%, 2% and 3% C addition to MgB_2

	0.1 mA				10 mA			
	$T_c(K)$	T_c onset(K)	T_c zero(K)	$\Delta T(K)$	$T_c(K)$	T_c onset(K)	T_c zero(K)	$\Delta T(K)$
0%C	27.07	28.18	24.17	4.01	25.85	31.42	23.19	8.23
1%C	28.7	32.31	24.92	7.39	27.78	32.62	25.29	7.33
2%C	29.45	30.48	26.82	3.66	28.14	33.01	25.16	7.85
3%C	32.48	35.21	30.19	5.02	31.67	36.92	29.7	7.22

It is difficult to obtain dense MgB_2 bulk samples because MgB_2 has very low fracture toughness and increase in C concentration also decreases fracture toughness of the pellets pressed to even lower values. For this study, pellets having C concentrations of 5% and 10 % were prepared but crumbled as soon as they are taken out of the cylindrical die.

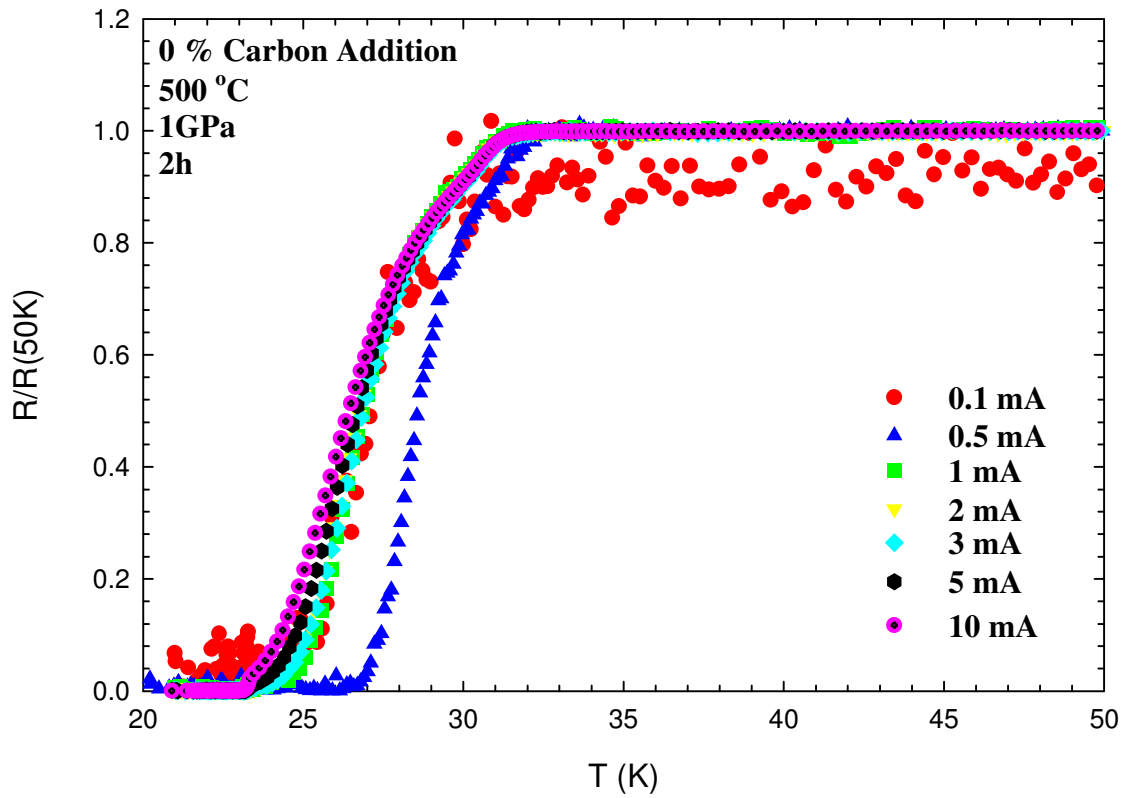


Figure 4.6. Normalized Resistance vs. Temperature plots of pellet with 0% C addition to MgB_2 .

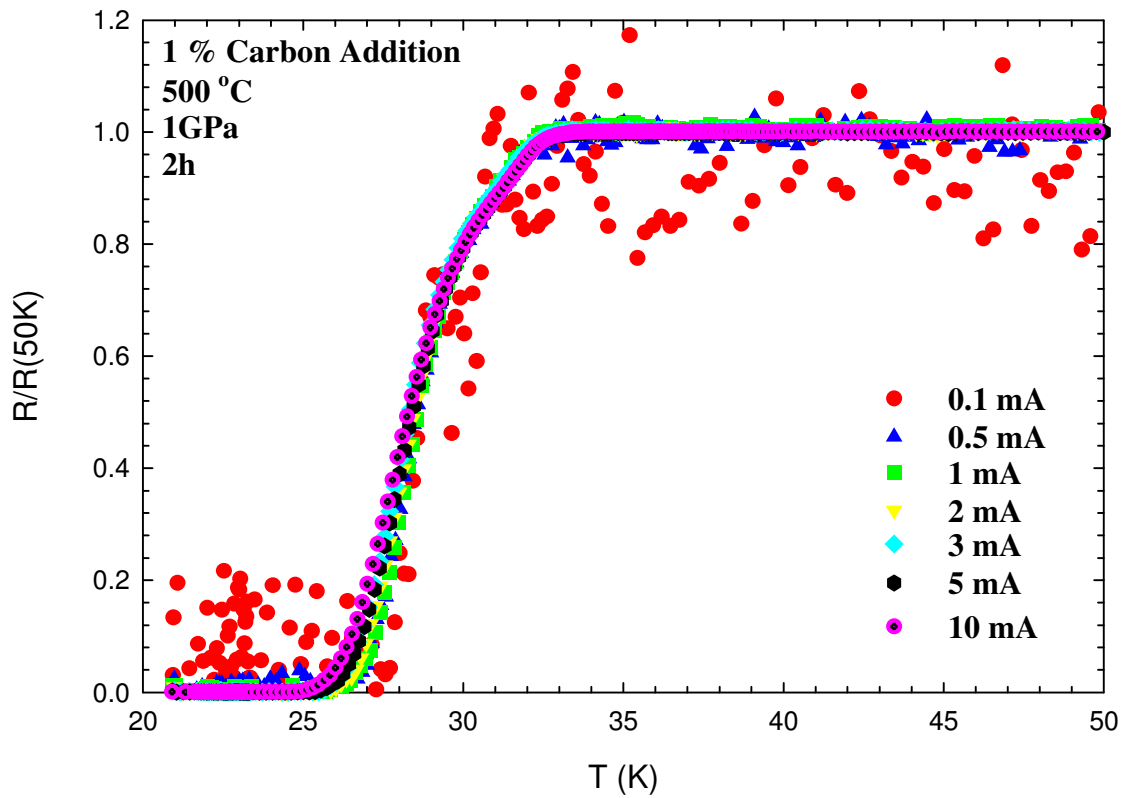


Figure 4.7. Normalized Resistance vs. Temperature plots of pellet with 1% C addition to MgB_2 .

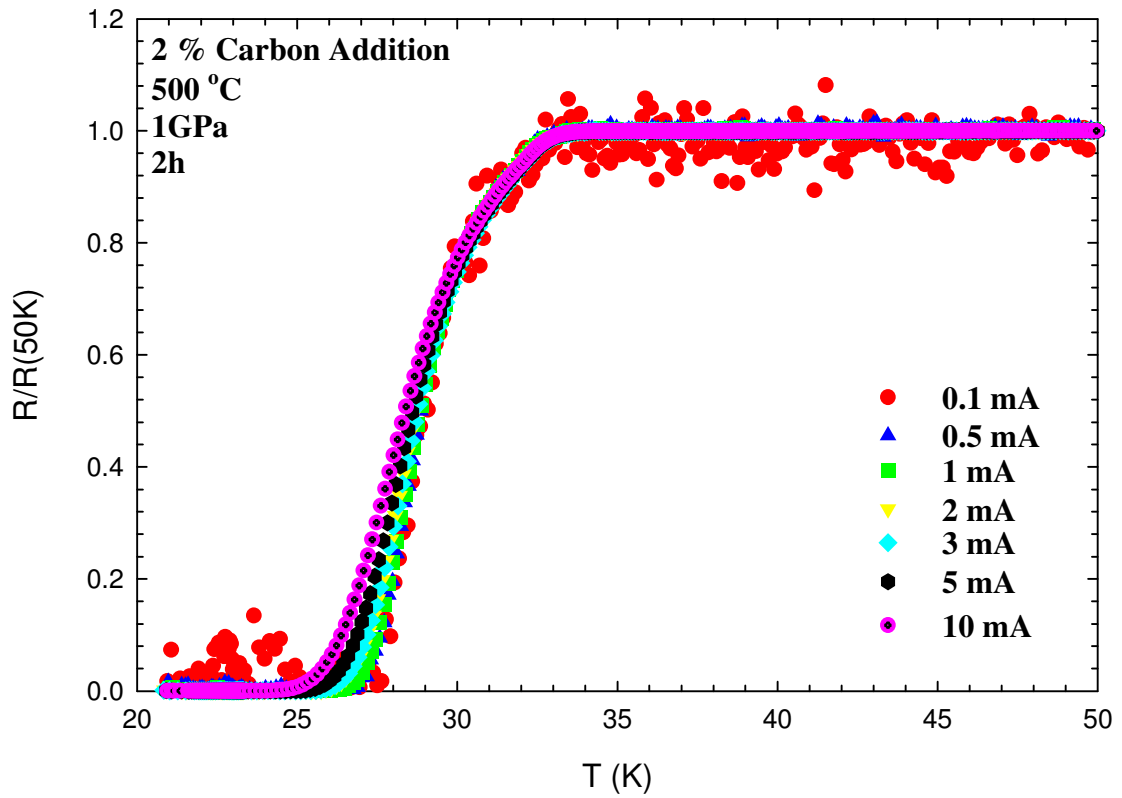


Figure 4.8. Normalized Resistance vs. Temperature plots of pellet with 2% C addition to MgB_2 .

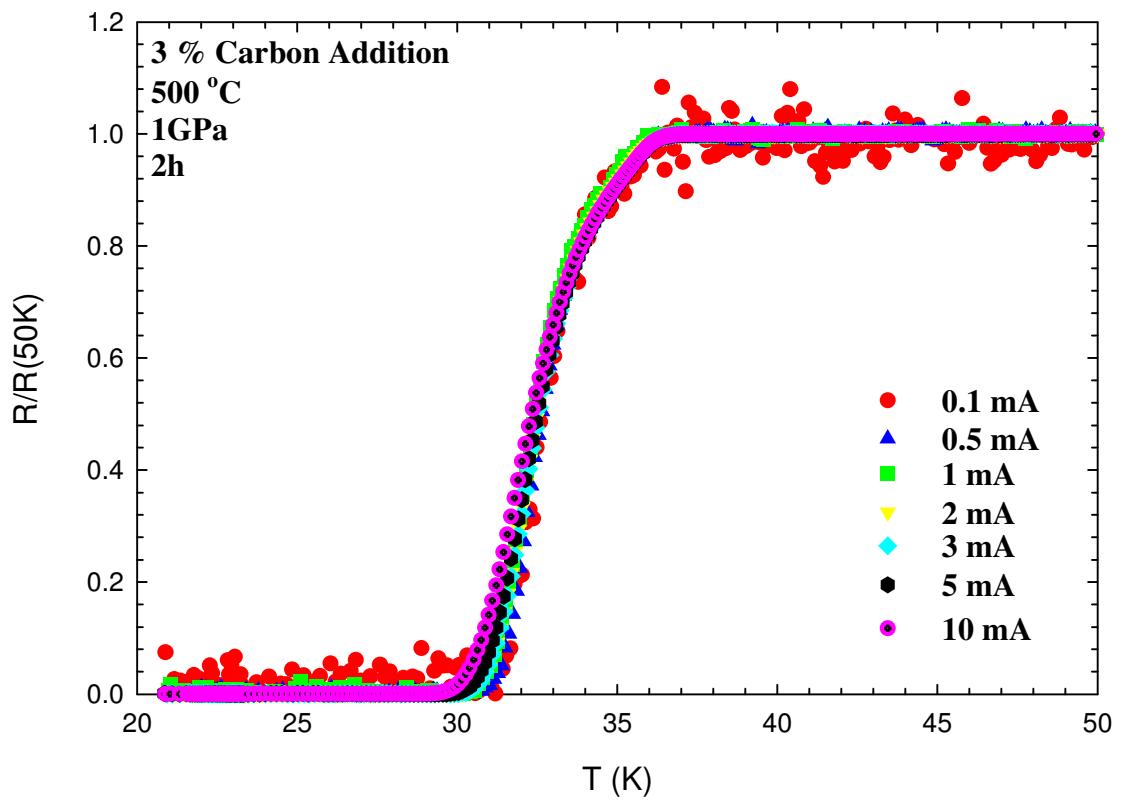


Figure 4.9. Normalized Resistance vs. Temperature plots of pellet with 3% C addition to MgB_2 .

Below, results for various C additions namely, 0%, 1%, 2% and 3% C additions for one applied current value are given. There are seven plots each representing a different applied current. The applied current values range from 0.1 mA to 10 mA. The measurement with 0.1 mA, as the current applied is very low, has noise compared to other measurements. In all plots there is an ordering of T_c 's depending on C concentration, 0% C having the lowest T_c value, and 3% C having the highest T_c value. Transition temperature of pellets having 1% C and 2% C concentration are between transition temperatures of 0% C and 3% C, and they are very close to each other. Transition temperature was found to increase with an increase in the C addition concentration. On the other hand, since C addition is studied in this thesis, it is hard to make a comparison with the C doping (or substitution) studies in literature. The literature for C doping or C substitution states that, as the C% increases, there is a decrease in the transition temperature of the specimens studied. The advantage of C as a material is although it decreases the transition temperature, it enhances the magnetic properties of the material. (Ribeiro et al. 2002b, Paranthaman et al. 2001, Bharathi et al. 2002) In this thesis our purpose was to see the effect of C addition to the electrical properties of MgB_2 .

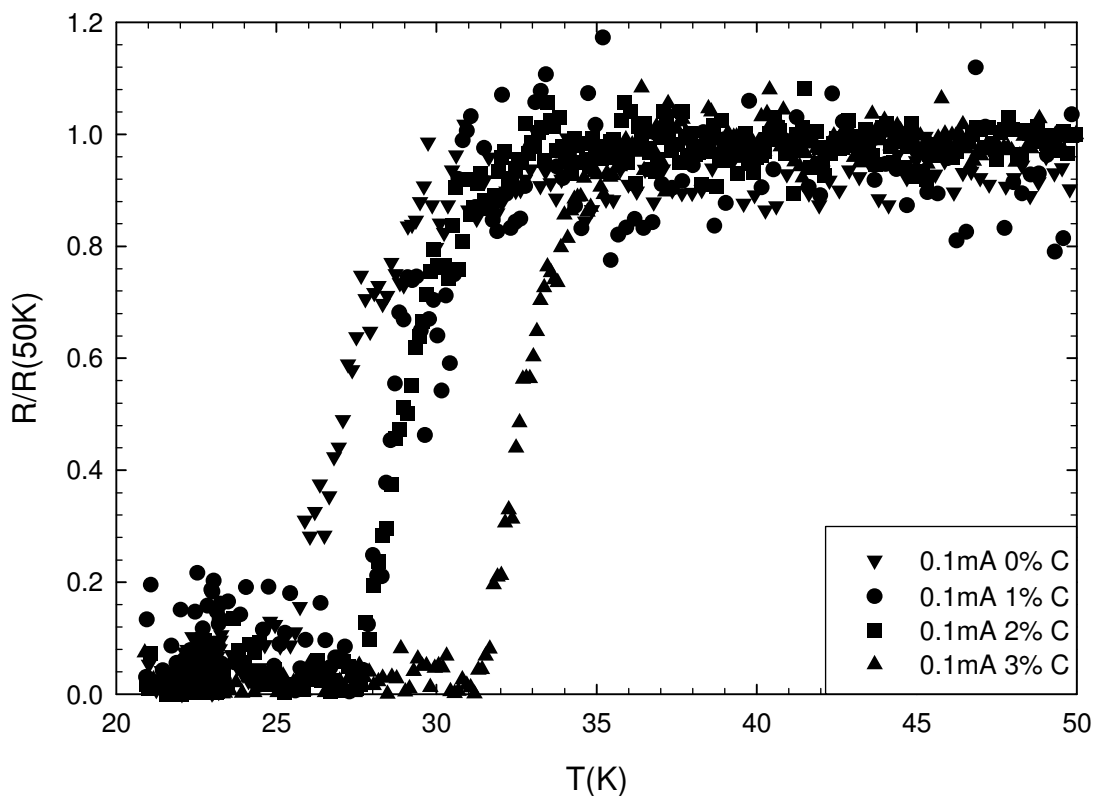


Figure 4.10. Normalized Resistance vs. Temperature plots of pellets with 0%, 1%, 2% and 3% C addition to MgB_2 with applied current 0.1 mA

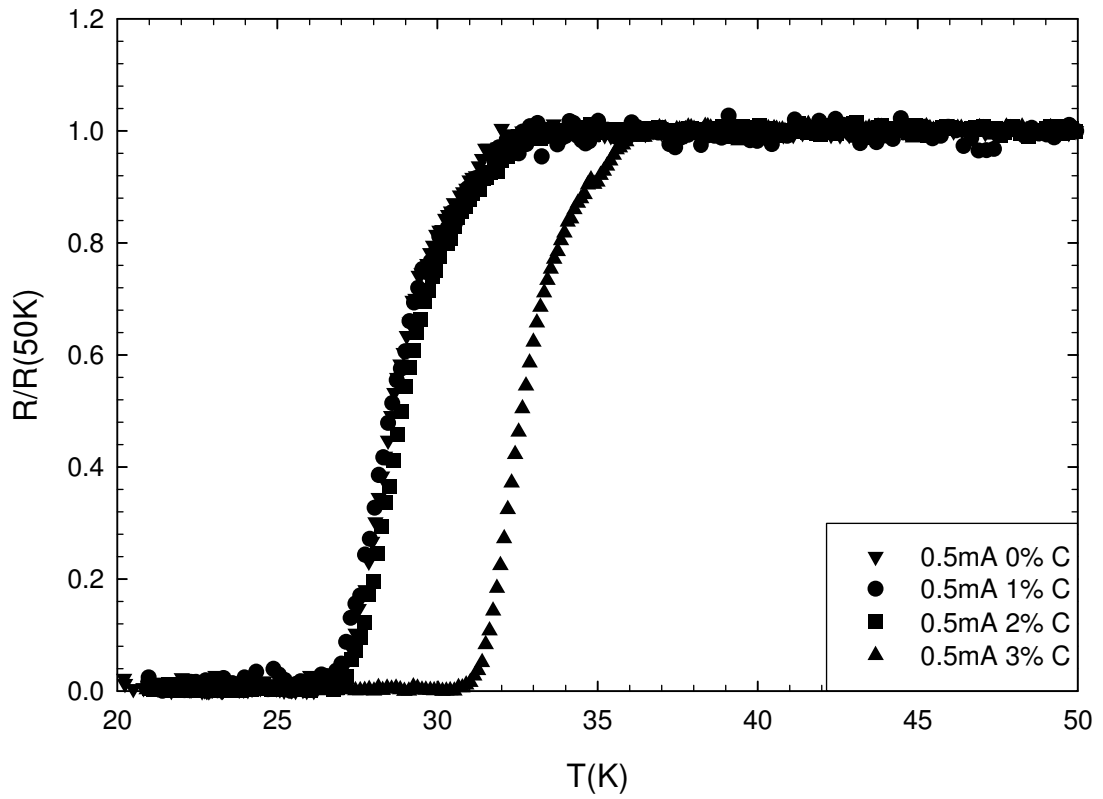


Figure 4.11. Normalized Resistance vs. Temperature plots of pellets with 0%, 1%, 2% and 3% C addition to MgB_2 with applied current 0.5 mA

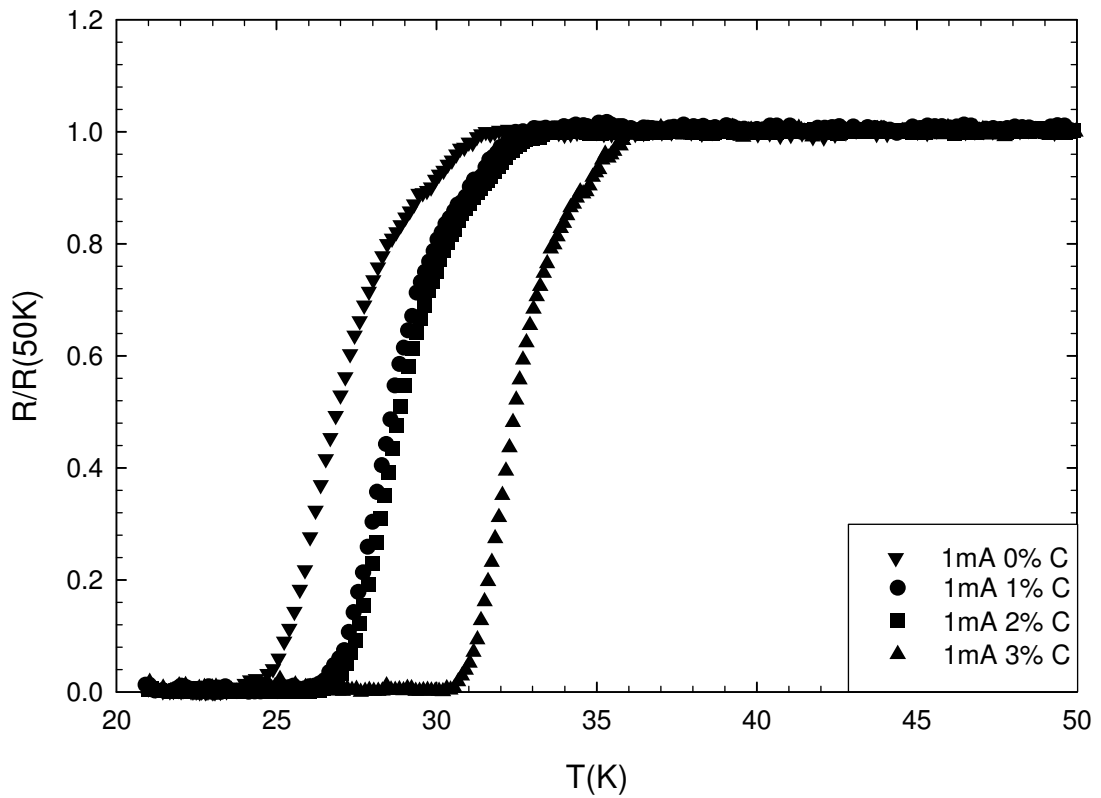


Figure 4.12. Normalized Resistance vs. Temperature plots of pellets with 0%, 1%, 2% and 3% C addition to MgB_2 with applied current 1 mA

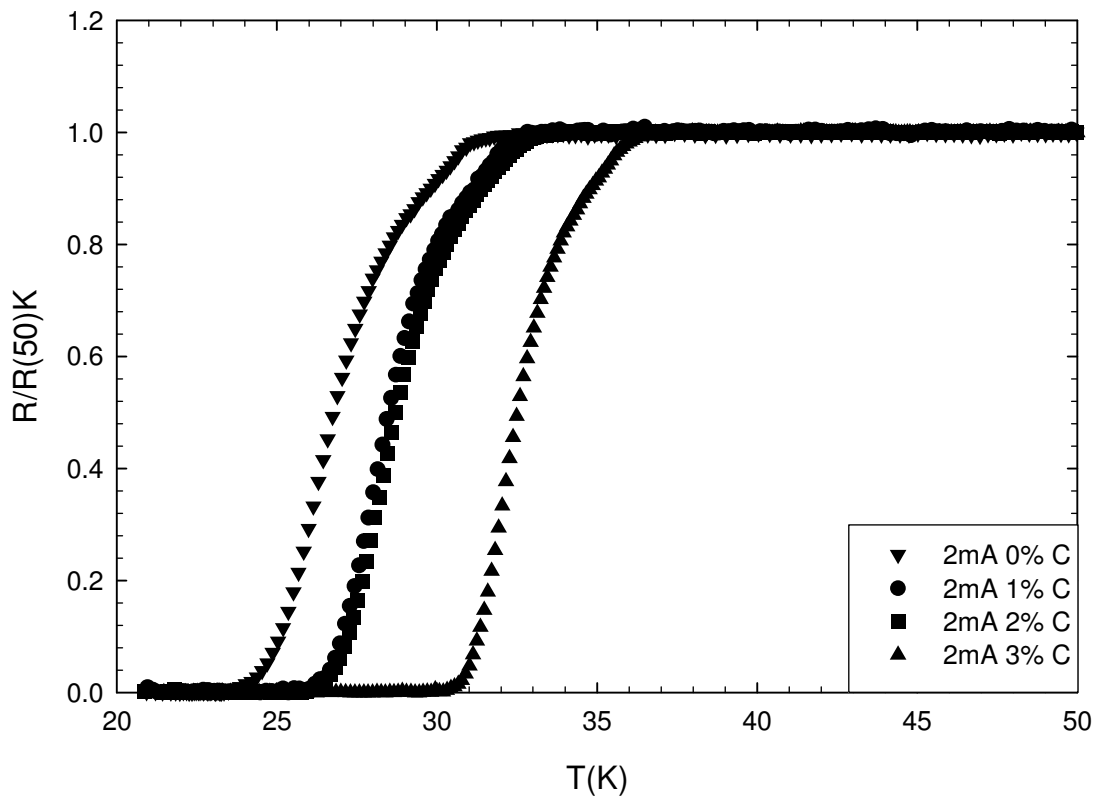


Figure 4.13. Normalized Resistance vs. Temperature plots of pellets with 0%, 1%, 2% and 3% C addition to MgB_2 with applied current 2 mA

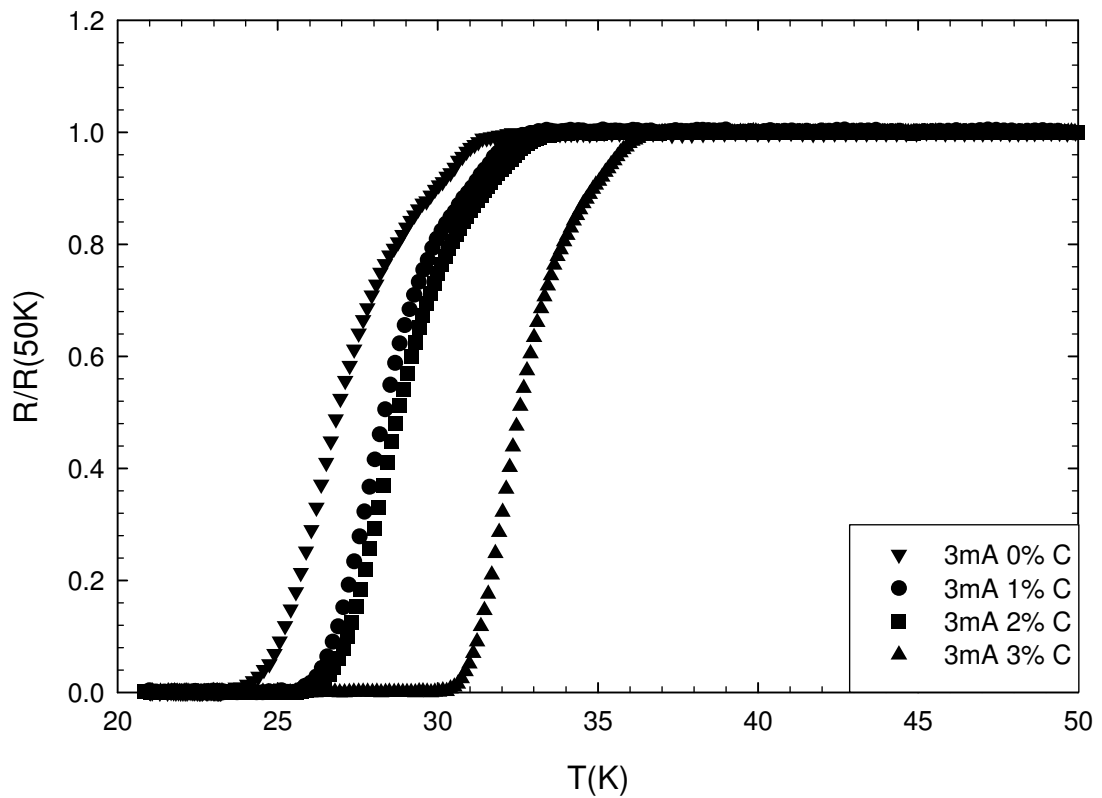


Figure 4.14. Normalized Resistance vs. Temperature plots of pellets with 0%, 1%, 2% and 3% C addition to MgB_2 with applied current 3 mA

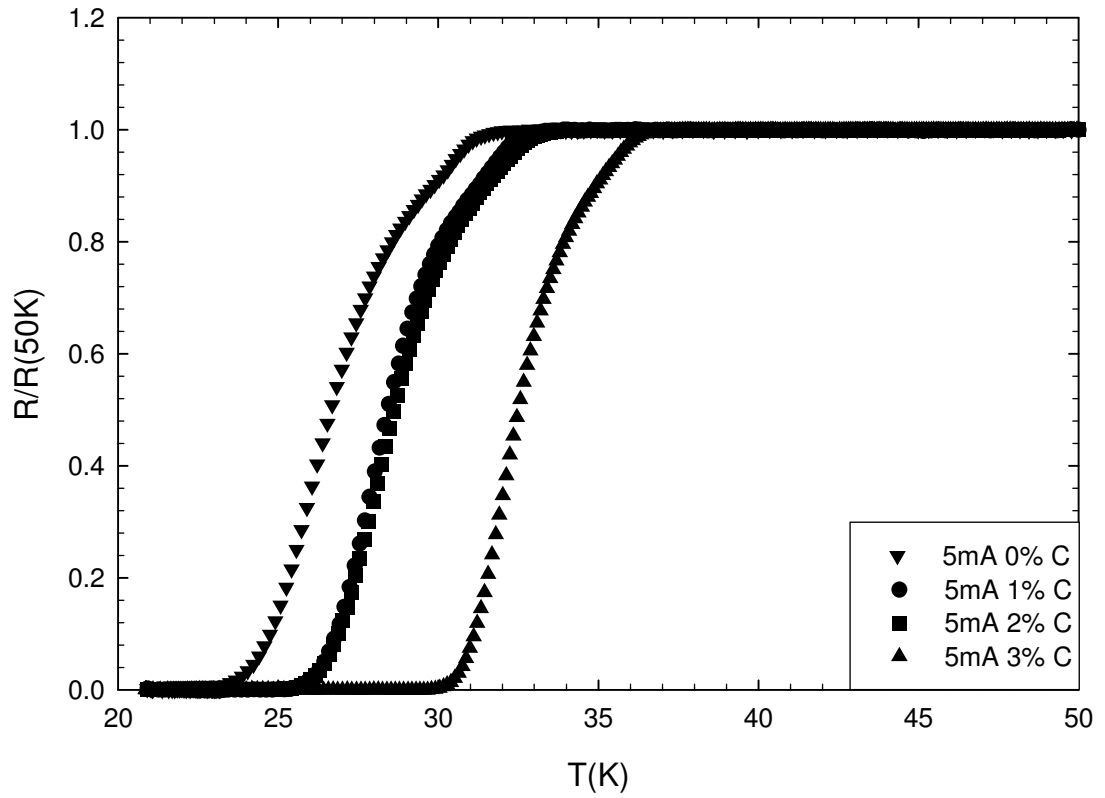


Figure 4.15. Normalized Resistance vs. Temperature plots of pellets with 0%, 1%, 2% and 3% C addition to MgB_2 with applied current 5 mA

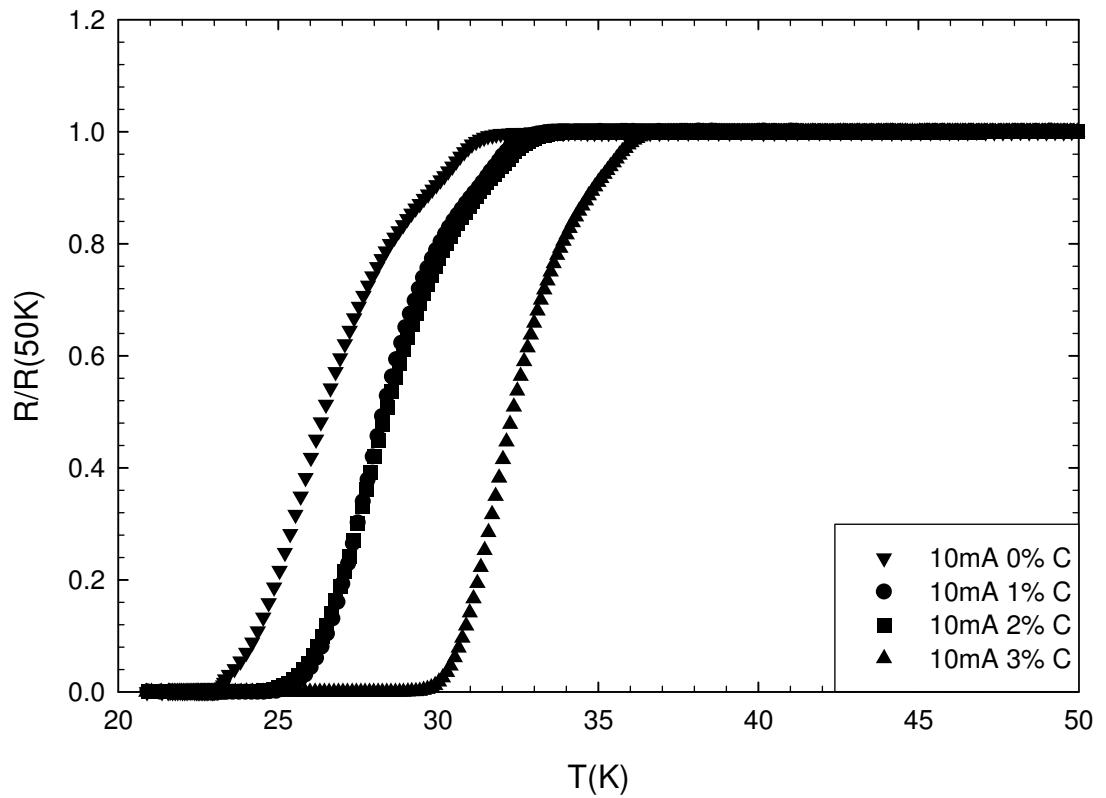


Figure 4.16. Normalized Resistance vs. Temperature plots of pellets with 0%, 1%, 2% and 3% C addition to MgB_2 with applied current 10 mA

4.3 Mg Added Cu Sheath MgB₂ Wires Prepared by PIT Method

Results

In this part of the study, superconducting MgB₂/Mg composite wires have been prepared by packing blend of MgB₂ and Mg powders inside of Cu tubes using powder in tube method to see the effect of Mg addition to Cu clad MgB₂ wires.

Blend of MgB₂ powder (-325 mesh) was filled into a Cu tube with a wall thickness of 1 mm and outer diameter of 5 mm in air. Only hand pressing was applied to densify the MgB₂ powder or Mg/MgB₂ mixture in Cu tube. The filled tube was cold drawn in a number of steps with about 5% of section reduction to a round Cu-clad MgB₂ wire with a core diameter of 0.7-0.8 mm and with an outer diameter of 1.5 mm, while the superconducting fill factor corresponds to about 25% - 30% for the whole conductor volume. The samples were then annealed in a tube furnace in a high purity Ar gas flow under ambient pressure at 800°C for 3 minutes and quenched to air for short annealing process. For longer annealing process, the samples were annealed at 400°C for 2 hours and kept in Ar gas flow until room temperature under ambient pressure.

We have analyzed the effect of cold working, annealing temperature and annealing time of the microstructure of the Cu-clad MgB₂ filaments of the wires by x-ray diffraction technique using Philips Expert Plus with Cu-K_α. The samples were prepared by removing the sheath material mechanically. The microstructure of the MgB₂ layers was investigated using a scanning electron microscope (SEM), Philips XL 30S Feg and energy dispersive x-ray diffraction (EDX).

Resistivity and critical current measurements were performed in a closed-cycle He refrigerator using four-probe method. R-T measurements were performed measuring the sample resistance during the heat up ramp. Temperature was controlled via calibrated low temperature RTD sensor in very close neighborhood to the sample. The critical current, I_c, measurements were performed at self magnetic field and it was evaluated with 1 μV/cm criterion. The current density (J_c) was obtained by dividing I_c by the cross-sectional area of the MgB₂ core, which was measured by optical microscopy.

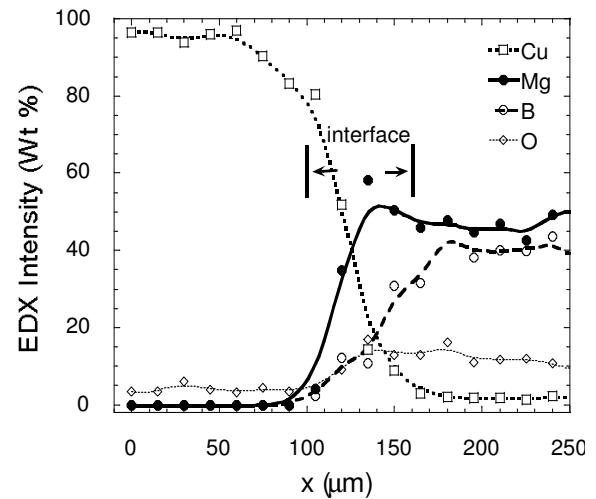
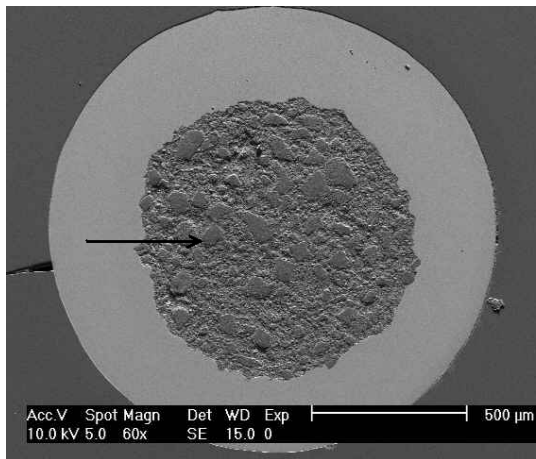


Figure 4.17. SEM micrograph of cross section of an annealed Cu-sheathed $\text{MgB}_2 + 5\%$ Mg composite wire with 1.5 mm in diameter. (on the left)

Figure 4.18. EDX Intensity has taken at the interface between Cu sheath and $\text{MgB}_2 + 5\%$ Mg core while moving along the radial direction toward to the core center as shown in Figure 4.17. The sample was prepared after cold drawing process and annealing at 800°C for 3 min. (on the right)

Figure 4.17 shows SEM picture of longitudinal cross section of a 1.5 mm in diameter of an annealed Cu-sheathed MgB_2 wire with 5% excess Mg. The diameter of the superconducting core has been measured about 0.8 mm from SEM picture. The formation of MgCu_2 interface layer on the Cu sheath wall is not so visible from the SEM picture taken using back-scattered electron imaging.

Figure 4.18 shows EDX Intensity taken at the interface between Cu sheath and MgB_2/Mg core while moving from Cu sheath to the $\text{MgB}_2 / 5\%$ Mg superconducting core about 250 μm along the radial direction as marked in Figure 4.17. The sample was prepared after cold drawing to 1.5 mm wire and annealing at 800°C for 3 min. The interface becomes clear extending from 100 μm to 150 μm from the starting point of the EDX scan of $15 \times 15 \mu\text{m}^2$ area. In this region, the amount of Cu decreases and Mg and B start to increase. It is clear that the stoichiometry of MgB_2 is not maintained and excess Mg and Cu are more pronounced. Mg and B ratio looks close to MgB_2 stoichiometry inside the superconducting core.

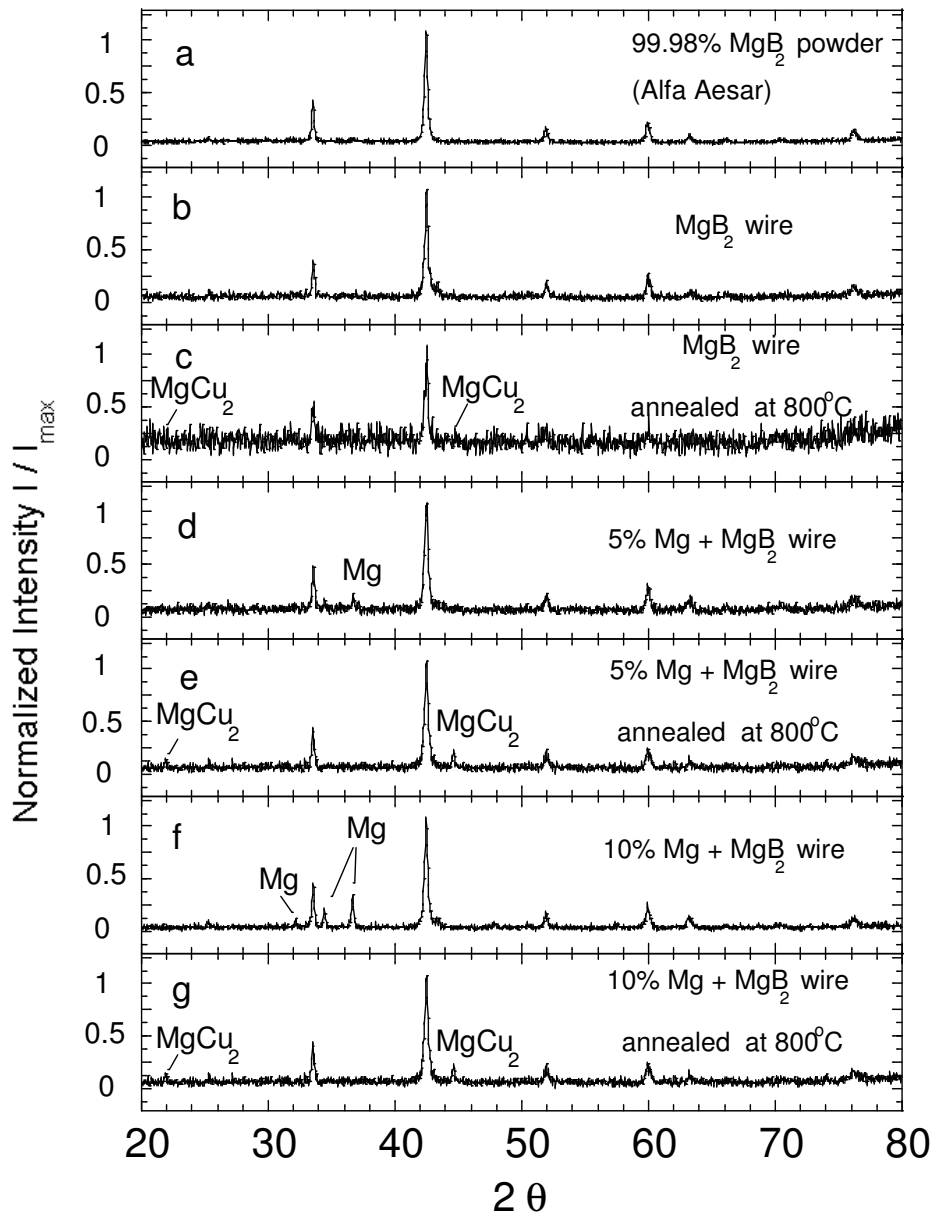


Figure 4.19. X-ray diffraction patterns of the MgB_2 powders, a) before packing, b) of the MgB_2 filament after removing the Cu sheath mechanically after the cold drawing process to a wire with outer diameter of 1.5 mm, c) after annealing at 800 °C for 3 min., d) of the mixed MgB_2 filament with 5% Mg before annealing, e) of the 5% Mg added filament after annealing at 800 °C for 3 min., f) of the mixed MgB_2 filament with 10% Mg before annealing, and g) of the 10% Mg added filament after annealing at 800 °C for 3 min.

The effect of cold working and annealing temperature and annealing time on the microstructural development of Cu-sheathed wires on the MgB_2 phase was analyzed by x-ray diffraction measurements as shown in Figure 4.19. The comparison of Figure 4.19c and Figure 4.19b shows Mg diffusion from pure MgB_2 superconducting core after annealing of Cu-clad MgB_2 wire at 800°C for 3 minutes. As a result, x-ray diffraction pattern in Figure 4.19c looks blur due to excess amorphous B in the core due to the loss of Mg during the formation of intermetallic MgCu_2 in the Cu sheath wall. After adding 5% excess Mg, unreacted Mg peaks become visible before annealing as shown in Figure 4.19d. After annealing, the excess Mg peaks disappear and MgCu_2 peaks can be seen in Figure 4.19e. This shows that most of the excess Mg was spent for the formation of MgCu_2 layer on the interface between Cu and MgB_2/Mg superconducting composite core. Similar peaks were observed for 10% Mg added composite wires except that the excess Mg peaks are more pronounced before annealing as seen in Figure 4.19f. They disappear after annealing at 800°C for 3 minutes as seen in Figure 4.19g and there is no sign of Mg saturation since none of the Mg is visible. This means MgCu_2 layer formation is still active. There is no sign of evident peak broadening or shifting that could be associated with molecular structural parameters of the MgB_2 phase inside Cu sheath.

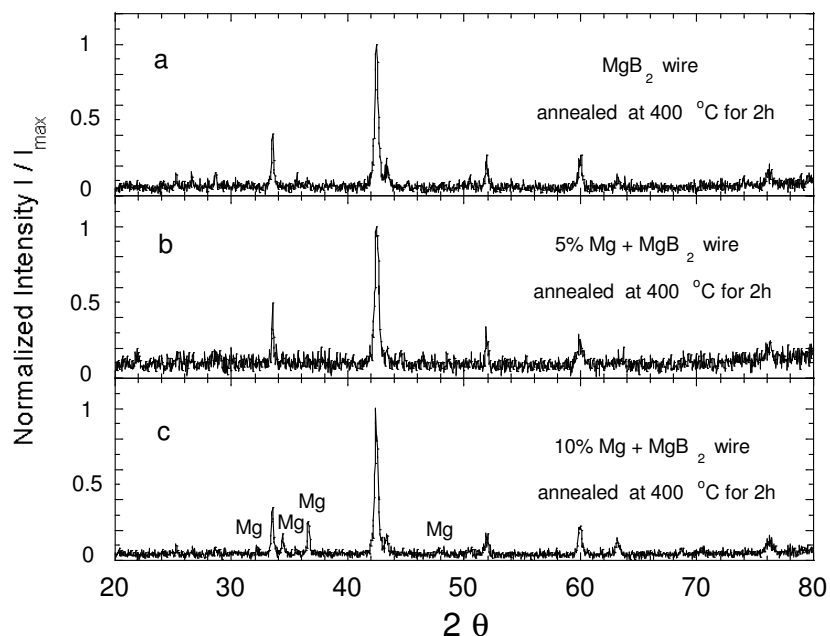


Figure 4.20. X-ray diffraction patterns a) of the MgB_2 (pure) filament of the Cu-clad MgB_2 wire after annealing at 400°C for 2 h, b) of the 5% Mg added filament after annealing at 400°C for 2 h, c) of the 10% Mg added filament after annealing at 400°C for 2 h.

We have not observed any evident peak for the MgCu_2 formation in the x-ray diffraction pattern of the MgB_2/Mg composite wires annealed at 400°C for 2 hours as shown in Figure 4.20. This means that there is no reaction between Mg and Cu sheath wall below the melting point of Mg, since the Mg peaks of the 10% Mg added filament still remain unchanged after annealing at 400°C for 2 h as seen in Figure 4.20c.

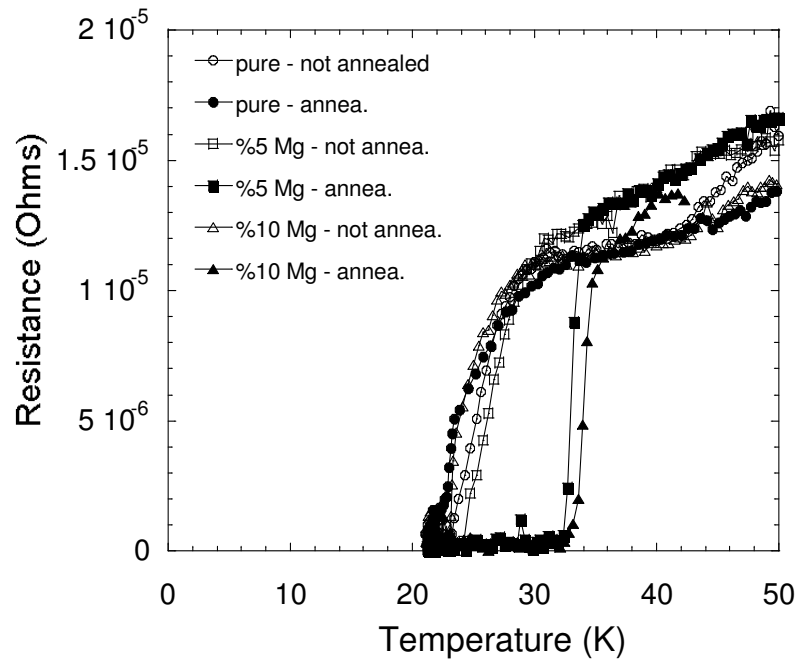


Figure 4.21. R-T characteristics of sintered and un-sintered MgB_2 wires with Cu sheath material at a driven current of 50 mA.

Figure 4.21 demonstrates resistance versus temperature characteristics of sintered and un-sintered wires made of MgB_2/Mg composite wires with outer diameter of 1.5 mm with Cu sheath at a driven current of 50 mA. T_c of the unsintered Cu-clad MgB_2/Mg composite wires increases from 26 K to 27 K by adding 5% Mg while it decreases to 25 K with 10% excess Mg. The change in T_c is approximately 5-6 K.

Similar improvements in T_c and J_c have been seen after annealing at 400°C for 2 hours or at 800°C for 3 minutes as the amount of excess Mg are increased in the MgB_2 core. T_c of the Cu-clad MgB_2 wire with 5% Mg increases from 27 K to 33.5 K with relatively sharp transition. T_c of the Cu-clad MgB_2 wire with 10% Mg shows better result and it increases from 25 K to 34.5 K, while T_c of the pure Cu-clad MgB_2 wire without Mg decreases from 26 K to 23 K. These confirm the XRD and EDX results discussed above. This means that there is degradation for the pure MgB_2 wires after annealing due to the

loss of Mg from the superconducting core, while excess Mg helps to maintain the stoichiometry of MgB₂ compound. For shorter sintering process, to decrease the formation of MgCu₂ layer in the interface, 3 minutes at 800°C is sufficient enough to reach to the same annealing effect on the MgB₂/Mg composite wires.

The formation of intermetallic MgCu₂ layer on the tube walls, and diffusion of Mg from the superconducting core into the interface between sheath and core was observed for the Cu-clad MgB₂/Mg composite wires annealed at 800°C. Temperature dependence of resistance and J_c measurements show that excess Mg gives better results at annealing at 400°C for 2 hours, for longer sintering process. For shorter sintering process, 3 minutes at 800°C is optimum value to reach to the same annealing effect on the MgB₂/Mg composite wires. Excess Mg prevents the degradation of MgB₂ superconducting core during the formation of MgCu₂ layer, which might prevent the diffusion of Mg from the superconducting core so that the stoichiometry of the MgB₂ is maintained. It was found that electronic properties of superconducting MgB₂ wires are improving with excess Mg and annealing temperature and time.

CHAPTER 5

CONCLUSIONS

The recent discovery of MgB_2 (2001) has aroused a great interest because of its high T_c (39 K). Furthermore, simple crystal structure, large coherence lengths, high critical current densities (J_c) and critical fields (B_{c2}), and transparency of grain boundaries to current promise that MgB_2 will be a good material for both large-scale applications and electronic device applications. Approximately 99% of the superconductor market depends on large-scale applications based on production of wires and tapes. MgB_2 suggests a higher operating temperature (20 K) than the current technology in use (Nb-based superconductors, 4.2 K). Therefore, production of wires from MgB_2 has great significance in terms of science and industry. However, MgB_2 is not a standalone material to produce wires because of its low fracture toughness. The widespread method for producing wires from brittle powders is Powder In Tube Method (PIT). Besides PIT method there is an alternate method for producing tapes, wires and bulk samples from brittle powders called Metal Matrix Composite Method (MMC).

This study consists of three main parts. In the first part of this thesis, elementary B synthesis, purification of this B, MgB_2 synthesis microstructural and electrical characterization of the pellet produced from synthesized MgB_2 is aimed. The importance of B for the MgB_2 production is clear, but purpose of our study is also supported by the fact that Turkey is very rich in B.

EDX analysis was carried out in order to detect Boron amount and purity in the produced amorphous powder. After repeating acid leaching process, EDX analysis of the produced powder given in Figure 4.1 shows that its purity is 93.5 % and Mg impurity is around 5 %. 5% Mg impurity in the amorphous Boron powder is not important, since the final goal is to obtain superconducting MgB_2 using another solid-state reaction of produced amorphous B powder with high purity commercial Mg. Reducing the amount of Mg by 5% in the solid-state reaction to obtain superconducting MgB_2 powder compensates this impurity of the B. The purity of obtained Boron increases with increasing number of acid leaching steps as shown in EDX analysis (Figure 4.1). Repeating the acid leaching steps has an important role in Boron purity.

The ratio of Boron in the initial output product is 6.97 %. Then it increases to 16 % after first acid leaching and it is above 80 % after 6th step. Finally, after 13th step, 93% of amorphous elementary B purity was reached.

XRD patterns of the 2B+MgO powders after the reaction of B₂O₃ and Mg at 800°C for 1 h in Ar atmosphere before and after acid leaching is shown in Figure 4.2. The peaks before acid leaching were changed into a noise showing only amorphous B after acid leaching process. This case shows all the phases except MgO and B in the sediment disappeared.

For the production of MgB₂ produced B powder is mixed with commercial Mg powder in stoichiometric ratios. XRD results show that the produced and commercial MgB₂ peaks matches exactly except a Mg peak present at $2\theta = 63.6$ as impurity.

SEM images of produced MgB₂ in powder form and in a pellet form are compared and the average particle size for the pellet is found to be smaller due to pressure and annealing.

Normalized resistance versus temperature plot for fabricated MgB₂ starting from B₂O₃ is analyzed. The produced superconducting MgB₂ pellet makes a transition at 32 K. It is measured that the density of the superconducting MgB₂ pellet was 1.99 g/cm³. This value is smaller than the theoretical value of MgB₂ of 2.62 g/cm³. This shows that there is large amount of voids present in the material. This high porosity ratio causes low grain connectivity between MgB₂ grains. The low transition temperature and broaden transition interval indicate low grain connectivity due to porosity in the material.

The XRD, EDX, SEM and temperature dependence of resistivity results revealed that superconducting MgB₂ is successfully produced from the reaction of Mg and B reduced from the B₂O₃. DC resistivity measurement was done to determine the superconducting properties of the produced powders. The produced superconducting MgB₂ pellet shows a T_c onset value of 32 K. There is a slight difference between T_c values of the pellet pressed from MgB₂ produced at IYTE, and the pellet pressed from commercial MgB₂. This difference which can be seen in Figure 4.5 is considered to be a result of impurities left in the material in the purification process of B.

In the second part, C added MgB₂ pellet production by MMC method is studied. Temperature dependence of resistance of C added MgB₂ pellets is investigated. In literature only C substitution or doping has been studied. According to there researches, the effect of C doping or substitution is found to be a decrease in the critical temperature

of the samples but on the other hand an enhancement is observed in the magnetic properties of the specimen. (Ribeiro et al. 2002b, Paranthaman et al. 2001, Bharathi et al. 2002). However in this study, a new approach C addition is applied to see the effect on T_c . The electrical characterization results with temperature dependence of resistance plots are discussed.

The plots reveal that as the deriving currents increase, the measurement becomes more reliable with less noise in data. But as expected, effect of joule heating can be seen, as the deriving current increases, T_c for the entire set of samples, shift to higher values.

In all plots there is an ordering of T_c 's depending on C concentration, 0% C having the lowest T_c value, and 3% C having the highest T_c value. Transition temperature of pellets having 1% C and 2% C concentration are between transition temperatures of 0% C and 3% C, and they are very close to each other. Transition temperature was found to increase with an increase in the C addition concentration.

In the last part of the study, superconducting MgB_2/Mg composite wires have been prepared by packing blend of MgB_2 and Mg powders inside of Cu tubes using powder in tube method to see the effect of Mg addition to Cu clad MgB_2 wires.

We have analyzed the effect of cold working, annealing temperature and annealing time of the microstructure of the Cu-clad MgB_2 filaments of the wires by x-ray diffraction technique using Philips Expert Plus with $Cu-K\alpha$. The samples were prepared by removing the sheath material mechanically. The microstructure of the MgB_2 layers was investigated using a scanning electron microscope (SEM), Philips XL 30S Feg and energy dispersive x-ray diffraction (EDX). Resistivity and critical current measurements were performed in a closed-cycle He refrigerator using four-probe method.

In the SEM picture of longitudinal cross section of a 1.5 mm in diameter of an annealed Cu-sheathed MgB_2 wire with 5% excess Mg the diameter of the superconducting core has been measured to be about 0.8 mm. EDX Intensity taken at the interface between Cu sheath and MgB_2/Mg core while moving from Cu sheath to the $MgB_2 / 5%Mg$ superconducting core about 250 μm along the radial direction shows the expected interface which becomes clear extending from 100 μm to 150 μm from the starting point of the EDX scan of $15 \times 15 \mu m^2$ area. In this region, the amount of Cu decreases and Mg and B start to increase. It is clear that the stoichiometry of MgB_2 is not

maintained and excess Mg and Cu are more pronounced. Mg and B ratio looks close to MgB_2 stoichiometry inside the superconducting core.

The effect of cold working and annealing temperature and annealing time on the microstructural development of Cu-sheathed wires on the MgB_2 phase was analyzed by x-ray diffraction measurements. The comparison of Figure 4.19c and Figure 4.19b shows Mg diffusion from pure MgB_2 superconducting core after annealing of Cu-clad MgB_2 wire at 800°C for 3 minutes. As a result, x-ray diffraction pattern in Figure 4.19c looks blur due to excess amorphous B in the core due to the loss of Mg during the formation of intermetallic MgCu_2 in the Cu sheath wall. After adding 5% excess Mg, unreacted Mg peaks become visible before annealing as shown in Figure 4.19d. After annealing, the excess Mg peaks disappear and MgCu_2 peaks can be seen in Figure 4.19e. This shows that most of the excess Mg was spent for the formation of MgCu_2 layer on the interface between Cu and MgB_2/Mg superconducting composite core. Similar peaks were observed for 10% Mg added composite wires except that the excess Mg peaks are more pronounced before annealing as seen in Figure 4.19f. They disappear after annealing at 800°C for 3 minutes as seen in Figure 4.19g and there is no sign of Mg saturation since none of the Mg is visible. This means MgCu_2 layer formation is still active. There is no sign of evident peak broadening or shifting that could be associated with molecular structural parameters of the MgB_2 phase inside Cu sheath.

There is not any evident peak for the MgCu_2 formation in the x-ray diffraction pattern of the MgB_2/Mg composite wires annealed at 400°C for 2 hours. This means that there is no reaction between Mg and Cu sheath wall below the melting point of Mg, since the Mg peaks of the 10% Mg added filament still remain unchanged after annealing at 400°C for 2 h.

Resistance versus temperature characteristics of sintered and un-sintered wires made of MgB_2/Mg composite wires with outer diameter of 1.5 mm with Cu sheath at a driven current of 50 mA show that the T_c of the unsintered Cu-clad MgB_2/Mg composite wires increases from 26 K to 27 K by adding 5% Mg while it decreases to 25 K with 10% excess Mg. The change in T_c is approximately 5-6 K.

Similar improvements in T_c and J_c have been seen after annealing at 400°C for 2 hours or at 800°C for 3 minutes as the amount of excess Mg are increased in the MgB_2 core. T_c of the Cu-clad MgB_2 wire with 5% Mg increases from 27 K to 33.5 K with relatively sharp transition. T_c of the Cu-clad MgB_2 wire with 10% Mg shows better result and it increases from 25 K to 34.5 K, while T_c of the pure Cu-clad MgB_2 wire without Mg

decreases from 26 K to 23 K. These confirm the XRD and EDX results discussed above. This means that there is degradation for the pure MgB_2 wires after annealing due to the loss of Mg from the superconducting core, while excess Mg helps to maintain the stoichiometry of MgB_2 compound. For shorter sintering process, to decrease the formation of MgCu_2 layer in the interface, 3 minutes at 800°C is sufficient enough to reach to the same annealing effect on the MgB_2/Mg composite wires.

The formation of intermetallic MgCu_2 layer on the tube walls, and diffusion of Mg from the superconducting core into the interface between sheath and core was observed for the Cu-clad MgB_2/Mg composite wires annealed at 800°C . Temperature dependence of resistance and J_c measurements show that excess Mg gives better results at annealing at 400°C for 2 hours, for longer sintering process. For shorter sintering process, 3 minutes at 800°C is optimum value to reach to the same annealing effect on the MgB_2/Mg composite wires. Excess Mg prevents the degradation of MgB_2 superconducting core during the formation of MgCu_2 layer, which might prevent the diffusion of Mg from the superconducting core so that the stoichiometry of the MgB_2 is maintained. It was found that electronic properties of superconducting MgB_2 wires are improving with excess Mg and annealing temperature and time.

REFERENCES

- Bardeen, J., Cooper, L.N., Schrieffer, J.R. 1957. "Microscopic Theory of Superconductivity", *Physical Review*. Vol. 106, p. 162.
- Bednorz, J.G. and Mueller, K.A. 1986. "Possible High T_c Superconductivity in the Barium-Lanthanum-Copper-Oxygen System", *Zeitschrift fuer Physik B: Condensed Matter*. Vol. 64, p. 189.
- Bharathi, A., Jemima Balaselvi, S., Kalavathi, S., Reddy, G.L.N., Sankara Sastry, V., Hariharan, Y. and Radhakrishnan, T.S. 2002. "Carbon Solubility and Superconductivity in MgB_2 ", *Physica C*. Vol. 370, p. 211.
- Bordet, P., Mezouar, M., Nunez-Regueiro, M., Monteverde, M., M. Nunez-Regueiro, D., Rogado, N., Regan, K.A., Hayward, M.A., He, T., Loureiro, S.M. and Cava, R.T. 2001. "Absence of a Structural Transition up to 40 GPa in MgB_2 and the Relevance of Magnesium Nonstoichiometry", *Physical Review B*. Vol. 64, p. 172502.
- Bouquet, F., Fisher, R.A., Phillips, N.E., Hinks, D.G. and Jorgensen, J.D. 2001. "Specific Heat of MgB_2 ", *Physical Review Letters*. Vol. 87, p. 047001.
- Bu, S.D., Kim, D.M., Choi, J.H., Giencke, J., Patnaik, S., Cooley, L., Hellstrom, E.E., Larbalestier, D.C., Eom, C.B., Lettieri, J., Schlom, D.G., Tian, W., Pan, X.Q. 2002. "Synthesis and Properties of C-Axis Oriented Epitaxial MgB_2 Thin Films", *Condensed Matter*. p. 0204004.
- Bud'ko, S.L., Petrovic, C., Lapertot, G., Cunningham, C.E. and Canfield, P.C. 2001. "Magnetoresistivity and Complete $H_{c2}(T)$ in MgB_2 ", *Physical Review B*. Vol. 63, p. 220503.
- Bud'ko, S.L., Lapertot, G., Petrovic, C., Cunningham, C.E., Anderson, N., and Canfield, P.C. 2001. "Boron Isotope Effect in Superconducting MgB_2 ", *Physical Review Letters*. Vol. 86, p. 1877.
- Buzea, C. and Yamashita, T. 2001. "Review of Superconducting Properties of MgB_2 ", *Superconductors, Science and Technology*. Vol. 14, No. 11, R115.
- Canfield, P.C., Finnemore, D.K., Budko, S.L., Ostenson, J.E., Lapertot, G., Cunningham, C.E., Petrovic, C. 2001. "Superconductivity in Dense MgB_2 Wires", *Physical Review Letters*. Vol. 86, p. 2423.
- Cava, R.J., Takagi, H., Batlogg, B., Zandbergen, H.W., Krajewski, J.J., Peck, W.F., van Dover, R.B., Felder, R.J., Siegrist, T., Mizuhashi, K., Lee, J.O., Eisaki, H., Carter S.A., Uchida, S. 1994. "Superconductivity at 23 K in Yttrium Palladium Boride Carbide", *Nature*. Vol. 367, p. 146.

- Choi, H.J., Roundy, D., Sun, H., Cohen, M.L. and Louie, S.G. 2002. "The Origin of the Anomalous Superconducting Properties of MgB₂", *Nature*. Vol. 418, p. 758.
- Dou, S.X., Soltanian, S., Horvat, J., Wang, X.L., Zhou, S.H., Ionescu, M., Liu, H.K., Munroe, P., Tomsic, M. 2002. "Enhancement of the Critical Current Density and Flux Pinning of MgB₂ Superconductor by Nanoparticle SiC Doping", *Applied Physics Letters*. Vol. 81, p. 3419.
- Dunand, D.C. 2001. "Synthesis of Superconducting Mg/MgB₂ Composites", *Applied Physics Letters*. Vol. 79, p. 4186.
- Egilmez, M., Gunel, A., Okur, S., Tanoglu, M., Ozyuzer, L. 2004. "Electrical and Microstructural Properties of Superconducting MgB₂/Mg Composites", *Key Engineering Materials*. Vol. 270, p. 1197.
- Eltsev, Y., Nakao, K., Lee, S., Masui, T., Chikumoto, N., Tajima, S., Koshizuka, N., Murakami, M. 2001. "Anisotropic Resistivity and Hall Effect in MgB₂ Single Crystals", *Physical Review B*. Vol. 66, p. 180504.
- Eom, C.B., Lee, M.K., Choi, J.H., Belenky, L., Song, X., Cooley, L.D., Naus, M.T., Patnaik, S., Jiang, J., Rikel, M., Polyanskii, A., Gurevich, A., Cai, X.Y., Bu, S.D., Babcock, S.E., Hellstrom, E.E., Labalestier, D.C., Rogado, N., Regan, K.A., Hayward, M.A., He, T., Slusky, J.S., Inumaru, K., Haas, M.K., Cava, R.J. 2001. "High Critical Current Density and Enhanced Irreversibility Field in Superconducting MgB₂ Thin Films", *Nature*. Vol. 411, p. 558.
- Feng, Y., Yan, G., Zhao, Y., Wu, X.J., Pradhan, A.K., Zhang, X., Liu, C.F., Liu, X.H. and Zhou, L. 2003. "High Critical Current Density in MgB₂/Fe Wires", *Superconductor Science and Technology*. Vol. 16, p. 682.
- Feng, Y., Zhao, Y., Sun, Y.P., Liu, F.C., Fu, B.Q., Zhou, L., Cheng, C.H., Loshizuka, N., Murakami, M. 2001. "Improvement of Critical Current Density in MgB₂ Superconductors by Zr Doping at Ambient Pressure", *Applied Physics Letters*. Vol. 79, p. 3983.
- Flukiger, R., Suo, H.L., Musolino, N., Beneduce, C., Toulemonde, P., Lezza, P. 2003. "Superconducting Properties of MgB₂ Tapes and Wires", *Physica C*. Vol. 385, p. 286.
- Gavaler, J.R., Janocko, M.A. and Jones, C.K. 1974. "Preparation and Properties of High-T_c Nb-Ge Films", *Journal of Applied Physics*. Vol. 45, p. 3009.
- Giunchi, G., Ceresara, S., Ripamonti, G., DiZenobio, A., Rossi, S., Chiarelli, S., Spadoni, M., Wesche, R., Bruzzone, P.L. 2002. "High Performance New MgB₂ Superconducting Hollow Wires", *Condensed Matter*. p. 0207488.
- Glowacki, B.A., Majoros, M., Vickers, M., Evetts, J.E., Shi, Y. and McDougall, I. 2001. "Superconductivity of Powder-In-Tube MgB₂ Wires", *Superconductor Science and Technology*. Vol. 14, p. 193.

- Goldacker, W. and Schlachter, S.I. 2002. "Influence of Mechanical Reinforcement of MgB₂ Wires on the Superconducting Properties", *Physica C*. Vol. 378, p. 889.
- Gunel, A. 2003. "Electrical and structural properties of MgB₂/Mg composites", *M.S. thesis*, Izmir Institute of Technology.
- Heinen, O. and Bhasin, K.B. 1991. "Superconductivity Applications for Infrared and Microwave Devices II (ed. V.)", *Proc. Inst. Soc. For Opt. Eng.*, Vol. 1477. SPIE
- Hinks, D.G., Claus, H., and Jorgensen, J. D. 2001. "The Reduced Total Isotope Effect and its Implications on the Nature of Superconductivity in MgB₂", *Nature*. Vol. 411, p. 457.
- Hinks, D.G., Jorgensen, J.D., Zheng, H., Short, S. 2002. "Synthesis and Stoichiometry of MgB₂", *Physica C*. Vol. 382, p. 166.
- Jung, C.U., Kim, H.-J., Park, M.-S., Kim, M.-S., Kim, J.Y., Du, Z., Lee, S.-I., Kim, K.H., Betts, J.B., Jaime, M., Lacerda, A.H., Boebinger, G.S. 2002. "Effects of Unreacted Mg Impurities on the Transport Properties of MgB₂", *Physica C*. Vol. 377, p. 21.
- Kamakura, H., Matsumoto, A., Fujii, H., Togano, K. 2001. "High Transport Critical Current Density Obtained for Powder-In-Tube-Processed MgB₂ Tapes and Wires Using Stainless Steel and Cu–Ni Tubes", *Applied Physics Letters*. Vol. 79, p. 2435.
- Kang, W.N., Jung, C.U., Kim, K.H.P., Park, M.S., Lee, S.Y., Kim, H.J., Choi, E.M., Kim, K.H., Kim, M.S., Lee, S.I. 2001. "Hole Carrier in MgB₂ Characterized by Hall Measurements", *Applied Physics Letters*. Vol. 79, p. 982.
- Kang, W.N., Kim, H.J., Choi, E.M., Kim, K.H.P., Lee, H.S., Lee, S.I. 2002. "Hall Effect in C-Axis-Oriented MgB₂ Thin Films", *Physical Review B*. Vol. 65, p. 134508.
- Kim, K.H.P., Choi, J.-H., Jung, C.U., Chowdhury, P., Lee, H.-S., Park, M.-S., Kim, H.J., Kim, J.Y., Du, Z., Choi, E.-M., Kim, M.-S., Kang, W.N., Lee, S.-I., Sung, G.Y., Lee, J.Y. 2002. "Superconducting Properties of Well-Shaped MgB₂ Single Crystals", *Physical Review B*. Vol. 65, p. 100510.
- Komori, K., Kawagishi, K., Takano, Y., Arisawa, S., Kumakura, H., Fukutomi, M., Togano, K. 2002. "Approach for the Fabrication of MgB₂ Superconducting Tape with Large In-Field Transport Critical Current Density", *Applied Physics Letters*. Vol. 81, p. 1047.
- Larbalestier, D.C., Cooley, L.D., Rikel, M.O., Polyanskii, A.A., Jiang, J., Patnaik, S., Cai, X.Y., Feldmann, D.M., Gurevich, A., Squitieri, A.A., Naus, M.T., Eom, C.B., Hellstrom, E.E., Cava, R.J., Regan, K.A., Rogado, N., Hayward, M.A., He, T., Slusky, J.S., Khalifah, P., Inumaru, K., and Haas, M. 2001. "Strongly Linked Current Flow in Polycrystalline Forms of the Superconductor MgB₂", *Nature*. Vol. 410, p. 186.

- Liu, A.Y., Mazin, I.I., Kortus, J. 2001. "Beyond Eliashberg Superconductivity in MgB₂: Anharmonicity, Two-Phonon Scattering, and Multiple Gaps", *Physical Review Letters*. Vol. 87, p. 087005.
- Lorenz, B., Meng, R.L., Chu, C.W. 2001. "High-Pressure Study on MgB₂", *Physical Review B*. Vol. 64, p. 012507.
- M. Eisterer, B.A. Glowacki, H.W. Weber, L.R. Greenwood, M. Majoros, 2002. "Enhanced Transport Currents in Cu-Sheathed MgB₂ Wires", *Superconductor Science and Technology*. Vol. 15, p. 1088.
- Masui, T., and Tajima, S., 2003. "Normal State Transport Properties of MgB₂", *Physica C*. Vol. 385, p. 91.
- Meissner, W. and Ochsenfeld, R. 1933. "Ein neuer Effekt bei eintritt der Supraleitfähigkeit / A new effect concerning the onset of superconductivity", *Naturwissenschaft*. Vol. 21, p. 787.
- Moon, S.H., Yun, J.H., Lee, H.N., Kye, J.I., Kim, H.G., Chung, W., Oh, B., "High Critical Current Densities in Superconducting MgB₂ Thin Films", *Applied Physics Letters*. Vol. 79, p. 2429.
- Nagamatsu, J., Nakagawa, N., Muranaka, T., Zenitani, Y., Akimitsu, J. 2001. "Superconductivity at 39K in Magnesium Diboride", *Nature*. Vol. 410, p. 63.
- Naito, M. and Ueda, K. 2004. "Growth and Properties of Superconducting MgB₂ Thin Films", *Condensed Matter Preprint*. p. 0402333.
- Onnes, K.H. 1911. "Further Experiments with Liquid Helium. D. On the Change of the Electrical Resistance of Pure Metals at very low temperatures.... V. The Disappearance of the Resistance of Mercury", *Proceedings of the Section of Sciences, Koninklijke Akademie van Wetenschappen Amsterdam*, (1911), Vol. 14, p. 113 (122b).
- Paranthaman, M., Thompson, J.R. and Christen, D.K. 2001. "Effect of Carbon-Doping in Bulk Superconducting MgB₂ Samples", *Physica C*. Vol. 355, p. 1.
- Pradhan, A.K., Shi, Z.X., Tokunaga, M., Tamegai, T., Takano, Y., Togano, K., Kito, H., Ihara, H. 2001, "Electrical Transport and Anisotropic Superconducting Properties in Single Crystalline and Dense Polycrystalline MgB₂", *Physical Review Letters*. Vol. 64, p. 212509.
- Ribeiro, R.A., Bud'ko, S.L., Petrovic, C., Canfield, P.C. 2002 "Effects of Stoichiometry, Purity, Etching and Distilling on Resistance of MgB₂ Pellets and Wire Segments", *Physica C*. Vol. 382, p. 194.
- Ribeiro, R.A., Bud'ko, S.L., Petrovic, C., Canfield, P.C. 2002. "Carbon Doping of Superconducting Magnesium Diboride", *Physica C*. Vol. 384, p. 227.

- Rowell, J.M., 2003. "The Widely Variable Resistivity of MgB₂ Samples", *Superconductor Science and Technology*. Vol. 16, p. R17.
- Schmidt, H., Zasadzinski, J.F., Gray, K.E. and Hinks, D.G. 2001. "Energy Gap from Tunneling and Metallic Sharvin Contacts onto MgB₂: Evidence for a Weakened Surface Layer", *Physical Review B*. Vol. 63, p. 220504.
- Serquis, A., Civale, L., Hammon, D.L., Coulter, J.Y., Liao, X.Z., Zhu, Y.T., Peterson, D.E., Mueller, F.M. 2003. "Microstructure and High Critical Current of Powder in Tube MgB₂", *Applied Physics Letters*. Vol. 82, p. 1754.
- Serquis, A., Civale, L., Hammon, L. 2003. "Hot Isostatic Pressing of Powder in Tube MgB₂ Wires", *Applied Physics Letters*. Vol. 82, p. 2847.
- Sharma, P.A., Hur, N., Haribe, Y., Chen, C.H., Kim, B.G., Guha, S., Cieplak, M.Z. and Cheong, S-W. 2001. "Percolative Superconductivity in Mg_{1-x}B₂", *Physical Review Letters*. Vol. 89, p. 167003.
- Soltanian, S., Wang, X.L., Kusevic, I., Babic, E., Li, A.H., Qin, M.J., Horvat, J., Liu, H.K., Collings, E.W., Lee, E. 2001. "High-Transport Critical Current Density Above 30 K in Pure Fe-Clad MgB₂ Tape", *Physica C*. Vol. 361, p. 84.
- Suo, H.L., Lezza, P., Uglietti, D., Beneduce, C., Abuacherli, V., Flukiger, R. 2002. "Transport Critical Current Densities and n Factors in Mono- and Multifilamentary MgB₂/Fe Tapes and Wires Using Fine Powders", *Applied Superconductivity*. in press.
- Testardi, L.R., Wernick, J.H., Royer, W.A. 1974. "Superconductivity with Onset above 23 K in Niobium-Germanium Sputtered Films", *Solid State Communications*. Vol. 15, p. 1.
- Tu, J.J., Carr, G.L., Perebeinos, V., Homes, C.C., Strongin, M., Allen, P.B., Kang, W.N., Choi, E-M, Kim, H-J, Lee, S-I 2001. "Optical Properties of c-Axis Oriented Superconducting MgB₂ Films", *Physical Review Letters*. Vol. 87, p. 277001.
- Wang, J., Bugoslavsky, Y., Berenov, A., Cowey, L., Caplin, A.D., Cohen, L.F., MacManus, Driscoll, J.L., Cooley, L.D., Song, X., Larbalestier, D.C. 2002. "High Critical Current Density and Improved Irreversibility Field in Bulk MgB₂ Made by a Scaleable, Nanoparticle Addition Route", *Applied Physics Letters*. Vol. 81, p. 2026.
- Xiao, H., Song, W.H., Du, J.J., Sun, Y.P. and Fang, J. 2003. "Preparation and Superconductivity of MgB₂/Cu Tapes", *Physica C*. Vol. 386, p. 593.
- Xu, M., Kitazawa, H., Takano, Y., Ye, J., Nishida, K., Abe, H., Matsushita, A., Tsujii, N., Kido, G. 2001. "Single Crystal MgB₂ With Anisotropic Superconducting Properties", *Applied Physics Letters*. Vol. 79, p. 2779.
- Yildirim, T. 2002. "The Surprising Superconductor" *Materials Today*. Vol. 5, p. 40.

- Zhao, G-M. 2002 "Unconventional Phonon-Mediated Superconductivity in MgB₂", *New Journal of Physics*. Vol. 4, p. 3.1.
- Zhao, Y., Feng, Y., Huang, D.X., Machi, T., Cheng, C.H., Nakao, K., Chikumoto, N., Fudamoto, Y., Koshizuka, N., Murakami, M. 2002. "Doping Effect of Zr and Ti on The Critical Current Density of MgB₂ Bulk Superconductors Prepared Under Ambient Pressure", *Physica C*. Vol. 378-381, p. 122.
- Zhao, Y., Huang, D.X., Feng, Y., Cheng, C.H., Machi, T., Koshizuka, N., Murakami, M. 2002. "Nanoparticle Structure of MgB₂ With Ultrathin TiB₂ Grain Boundaries", *Applied Physics Letters*. Vol. 80, p. 1640.